Driving and Reversible Controlling of Motor Proteins by Photochromic Non-nucleoside Triphosphates.

[フォトクロミック非ヌクレオシド三リン酸によるモータータンパク質の駆動および可逆的制御]

A Thesis

Submitted for the Degree of

Doctor of Life Science

By

Nishad Perur

Laboratory of Smart Molecule

Transdisciplinary Life Science Course

Graduate School of Life Science

Hokkaido University

Japan, 2013

Dedicated to my parents and family…

DECLARATION

I hereby declare that the matter embodied in this thesis entitled **"Driving and Reversible Controlling of Motor Proteins by Photochromic Non-nucleoside Triphosphates"** is the result of investigations carried out by me under the supervision of ***Prof. Nobuyuki Tamaoki*** at the Laboratory of Smart Molecule, Transdisciplinary Life Science Course, Graduate School of Life Science, Hokkaido University, Japan and it has not been submitted elsewhere for the award of any degree or diploma.

In keeping with the general practice of reporting scientific observations, due acknowledgement has been made whenever the work described has been based on the findings of the other investigators. Any omission that might have occurred by oversight or error of judgments is regretted.

Nishad Perur

CERTIFICATE

I hereby certify that the work described in this thesis entitled **"Driving and Reversible Controlling of Motor Proteins by Photochromic Non-nucleoside Triphosphates"** has been carried out by ***Nishad Perur***, under my supervision at the Laboratory of Smart Molecule, Transdisciplinary Life Science Course, Graduate School of Life Science, Hokkaido University, Japan.

Prof. Nobuyuki Tamaoki

(Research Supervisor)

CONTENTS

1. Introduction

A huge amount of biological research in recent decades has led to the realization that the living cell can be viewed as a miniature factory that contains a large collection of dedicated motor proteins. These cytoskeletal motor proteins use the energy of adenosine triphosphate (ATP) hydrolysis to perform mechanical tasks such as cell division, cell motility (migration), intracellular transport, muscle contraction, and organization of the organelles within the cell.[1]

There are two classes of biomolecular motors: linear and rotary. Linear motors include the kinesin,[2] dynein[3] and myosin[4] motors while the rotary motors include the F_0-F_1 ATP synthase.[5] Kinesin and dynein are microtubule-based motor proteins that actively transport material throughout the cell. Kinesin walks along microtubules toward the plus ends, facilitating material transport from the cell interior toward the cortex. Dynein transports material toward the microtubule minus ends, moving from the cell periphery to the cell interior. Myosin motors act upon actin filaments to generate cell surface contractions and other morphological changes, as well as vesicle motility, cytoplasmic streaming and muscle cell contraction. These cytoskeletal motor proteins use the hydrolysis of adenosine triphosphate (ATP) to perform mechanical work with a remarkable degree of efficiency. The motor proteins associate with their filament tracks

through a “head” region, or motor domain, that binds and hydrolyzes ATP. Through a mechanochemical cycle of filament binding, conformational change, filament release, conformational relaxation, and filament rebinding, the motor protein and its associated cargo move one step at a time along the filament. ATP synthase is the universal protein that terminates oxidative phosphorylation by synthesizing ATP from ADP and phosphate. ATP synthase utilizes the energy stored in the electrochemical gradient across a membrane, to drive nucleotide synthesis. Remarkably, this process can be reversed in certain circumstances: ATP hydrolysis can drive the engine backwards so that ATP synthase functions as a proton pump. The latest advances in the field of biomolecular motors in nanotechnology have made it clear that these motor proteins possess a number of intrinsic characteristics that make them exquisite candidates for powering or manipulating nanoscale engineered devices.[6]

An important demand in the nanotechnology is artificial controlling of the activities of motor proteins. In an effort to control the activity of biomolecular motors, various methodologies have been developed so far. These include (1) the engineering of Zn^{2+} binding sites into ATP synthase motors and using the modulation of Zn^{2+} availability to govern the on / off state of the motor,[7] and (2) adding and removing inhibitors (such as the anesthetic lidocaine) can be used to inhibit or restore the

movement of kinesin on microtubules filament.[8] Although each method has shown promise to control motor protein activity, these approaches have not yet clearly demonstrated the ability to reversibly control motor activity over several cycles of activation.

When considering the biodevices, light-control would be most favorable because light has several advantages over other external stimuli such as high temporal and spatial resolution. Light can be applied to the targeted site without any physical contact and act without producing chemical waste. Hess *et al*. described the use of light and an inhibitor for the reversible controlling the movement of kinesin, accomplished by exploiting a UV-induced release of caged ATP.[9] But the accumulation waste products by the addition of inhibitor can reduce the efficiency of reversible controllability of the system. Photochromic molecules are known as the reversible light responsive compounds changing the properties of functional molecule. Azobenzene is one of the most studied photochromic compounds because it undergoes *cis*-to-*trans* photoisomerization that can be switched at particular wavelengths of light. This light-induced interconversion allows systems incorporating azobenzenes to be used as photo-switches, effecting rapid and reversible control over a variety of chemical, mechanical, electronic, and optical properties. Examples of azobenzene-based

photo-control have been demonstrated in photoswitchable phase changes,[10] phase separation (or reversal of phase separation),[11] solubility changes[12] and crystallization.[13]

Tamaoki *et al*. have been reported a photoisomerizable azobenzene monolayer surface to control the motility of kinesin motor reversibly upon alternating irradiations of UV and visible light.[14] It is an interesting challenge to regulate the activities of these motor proteins by controlling the energy supply. Recently, Tamaoki *et al*. synthesized ATP analogues substituted with an azobenzene unit at the ribose group and used them to drive and reversibly photocontrol the kinesin-microtubule motility system; the observed change in the motility upon photoirradiation of the ATP analogue was, however, far from satisfactory.[15] Our interest here is to design a novel photochromic non-nucleoside triphosphate to drive and control the activities of motor proteins in a repeated and reversible manner.

In this dissertation, a set of non-nucleoside triphosphates to drive and control the activities of motor proteins have been described. Among these, a novel azobenzene triphosphate has been demonstrated as an efficient substrate for motor proteins. The *cis-trans* photoisomerization of azobenzene moiety controls the activities of motor proteins reversibly and repeatedly.

2. Experimental section

2.1 Materials.

Unless otherwise noted, reagents and solvents were used as received from commercial sources without further purification. Column chromatography was performed on silica gel (60N, spherical, neutral, 40-50 μm), which was purchased from Kanto Chemicals. The ion exchange chromatography was carried out on DEAE Sephadex A-25 packing material, which was purchased from GE Healthcare.

2.2 General methods, instrumentation and measurements.

^{1}H NMR and ^{13}C NMR were measured at ECX-400 (400 MHz) (JEOL). ^{1}H NMR measurements were carried out using $CDCl_3$, CD_3OD and D_2O as solvents and tetramethylsilane (TMS) as an internal standard. For ^{13}C NMR spectrum, D_2O was used as solvent and methanol as an internal standard. Chemical shift data are given in units of parts per million (ppm) relative to TMS (for ^{1}H NMR spectra) and methanol (for ^{13}C NMR). Splitting patterns are denoted as s (singlet), d (doublet), t (triplet), m (multiplet), dd (doublet of doublet) or br (broad). Mass specta were measured using MALDI-TOF MS (Applied Biosystems Voyager DE Pro) and AccuTOF (JMS-T100LC) (JEOL). Absorption spectra were recorded using Agilent 8453 spectrophotometer.

Photoisomerization studies were conducted using a mercury/xenon lamp with suitable filters (366 nm and 436 nm). Microtubule motility assay was performed using an inverted fluorescence optical microscope (Olympus BX50) equipped with UPlan F1 100x/1.30 oil C1 objective lens (Olympus), appropriate filters; 630 nm excitation filter, neutral density filter (ND-25, 25 % transmission), an EBCCD color video camera (HAMAMATSU C7190), and the image processing system AQUACOSMOS (HAMAMATSU). In case of actomyosin motility assay, 520 nm excitation filter was used. Motility videos were analyzed using ImageJ software. The assay was performed at room temperature (22-23°C).

2.3 Synthesis section.

2.3.1 Synthesis of NPhAETP.

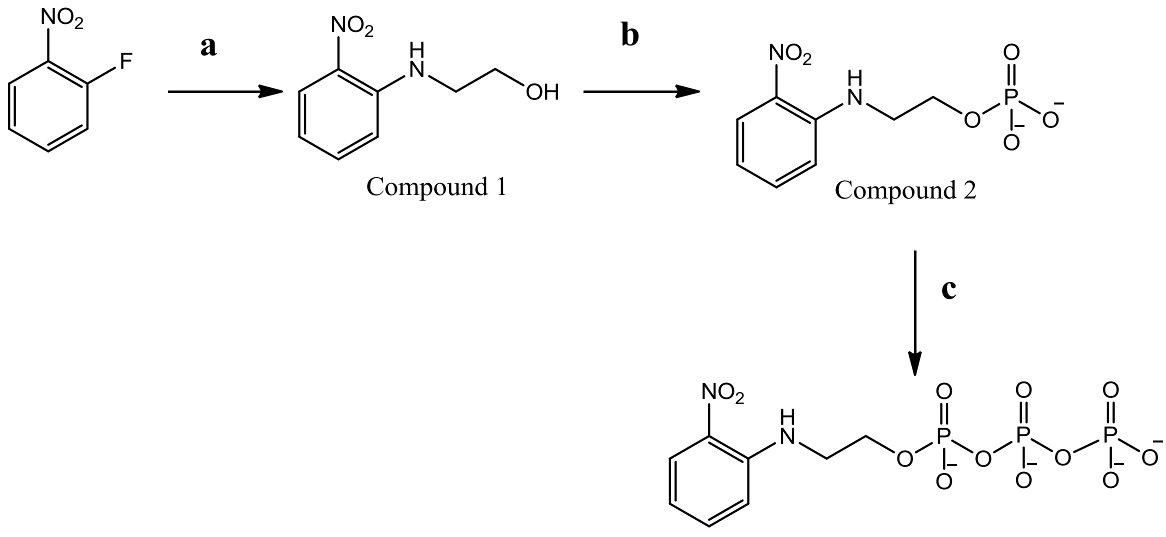

Synthetic scheme of NPhAETP: **a**) Ethanolamine, DMF, rt, overnight. **b**) $POCl_3$, Triethylphosphate, NaOH, rt, overnight. **c**) Tributylamine, Carbonyldiimidazole, Pyrophosphate, dry DMF, Ar atmosphere, rt, overnight.

Compound 1

To a solution of 1-fluoro-2-nitrobenzene (3.0 g, 21.3 mmol) in DMF (15 ml), ethanolamine (2.4 ml, 39 mmol) was added with stirring. The resultant solution was stirred for overnight. The reaction mixture was extracted with ethyl acetate/NaCl solution. The organic portion was dried over $MgSO_4$ and evaporated in a rotary

evaporator and obtained pure crystals of product in 91 % yield (3.52g). ^{1}H-NMR [$CDCl_3$ (TMS)]- δ= 1.69 (1H, t, J= 5.3 Hz), 3.50-3.54 (2H, m), 3.93-3.97 (2H, m), 6.68 (1H, t, J= 7.8 Hz), 6.9 (1H, d, J= 8.6 Hz), 7.45 (1H, t, J= 7.9 Hz), 8.19 (1H, d, J= 8.6 Hz), 8.24 (1H, br). ESI-MS: *m/z* = 183.58 [$M+H^+$] (calcd. 183.08).

Compound 2

A solution of $POCl_3$ (2.3 ml, 25 mmol) in triethylphosphate (16 ml) was placed in an ice bath and kept at 0° C under nitrogen condition. The solution was stirred vigorously while compound1 (3 g, 16.5 mmol) was added slowly in small quantities. The reaction was allowed to proceed for overnight at 0° C. Unreacted POCl3 was removed by rotary evaporation at 30° C. While the solution was stirred vigorously at 0° C, 10 ml of 4N NaOH was added dropwise to hydrolyze the acid chloride. Cold water (70 ml, 4° C) was added and the pH was adjusted to 7.5 with 6M NaOH. Then, the compound was purified by reverse-phase column chromatography using COSMOSIL C18-OPN packing material (Methanol/ Water, 1.5:8.5). The purified compound was applied to a DEAE-Sephadex A-25 column (2.5x30 cm, 20g) and eluted with 0.7 M triethylammonium hydrogencarbonate solution at 4°C. The eluted portion was evaporated with ethanol several times to remove triethyl ammonium hydrogencarbonate. Yield= 5.8% (0.25 g). ^{1}H-NMR [D_2O (TMS)]. δ= 3.69 (2H, t, J=

5.8 Hz), 4.10-4.17 (2H, m), 6.76 (1H, t, J= 7.6 Hz), 7.11 (1H, d, J= 8.8 Hz), 7.57 (1H, t, J= 7.8 Hz), 8.16 (1H, d, J= 8.8 Hz). ESI-MS: *m/z* = 261.47 [M-H^+] (calcd. 261.15).

Compound 3.

The triethylammonium salt of compound 3 (0.15 g, 0.57 mmol) is converted in to tributylammonium salt by the addition of tributylamine (0.29 ml, 1.1 mmol) in dry methanol (2 ml). Triethylamine and methanol were removed by rotary evaporation. The obtained tributylammonium salt was dissolved in dry DMF (3 ml). While stirring, 1,1'-carbonyldiimidazole (0.09 g, 0.59 mmol) dissolved in 0.8 ml of dry DMF was added under argon condition and the reaction was allowed to proceed for 18 hrs at room temperature. Excess 1,1'-carbonyldiimidazole was destroyed by addition of dry methanol (0.03 ml) and stirred for 1 hr. This solution was added dropwise with mixing to tributylammonium salt of pyrophospahate [which was prepared from tetrasodium pyrophosphate, 0.62 g, 1.32 mmol, as mentioned in the **section 2.3.4**] dissolved in dry DMF (2.6 ml). After reacting overnight at room temperature, the reaction mixture above was cooled to 0°C in an ice bath. Cold water (3 ml, 4°C) was added with mixing and the pH was brought to 7.5 with 1 M NaOH. Then the reaction mixture was extracted against ether/water mixture and water part was evaporated with ethanol at 30°C and dried. The dried residue was dissolved in 0.1 M triethylammonium hydrogencarbonate solution

and applied to a DEAE-Sephadex A-25 column(2.5x30 cm, 20g) and eluted with a linear 0.1-1.0 M (total volume 1 litre) triethylammonium hydrogencarbonate gradient at 4°C. The major peak of compound 4 was eluted at 0.69 M-0.77 M (10 ml/tube). The collected fractions were confirmed by ESI-mass and evaporated with ethanol several times to remove triethylammonium hydrogencarbonate. The obtained product is converted to the sodium salt using 1M NaI-acetone [see **section 2.3.5**]. Yield = 50 % (0.12g). ^{1}H-NMR [D_2O (TMS)]. δ= 3.73 (2H, t, J= 5.8 Hz), 4.21-4.26 (2H, m), 6.75 (1H, t, J= 7.6 Hz), 7.17 (1H, d, J= 8.8 Hz), 7.59 (1H, t, J= 7.8 Hz), 8.16 (1H, d, J= 8.8 Hz). ESI-MS: *m/z* = 420.92 [M-H^+] (calcd. 420.97).

2.3.2 Synthesis of NPhAdMTP.

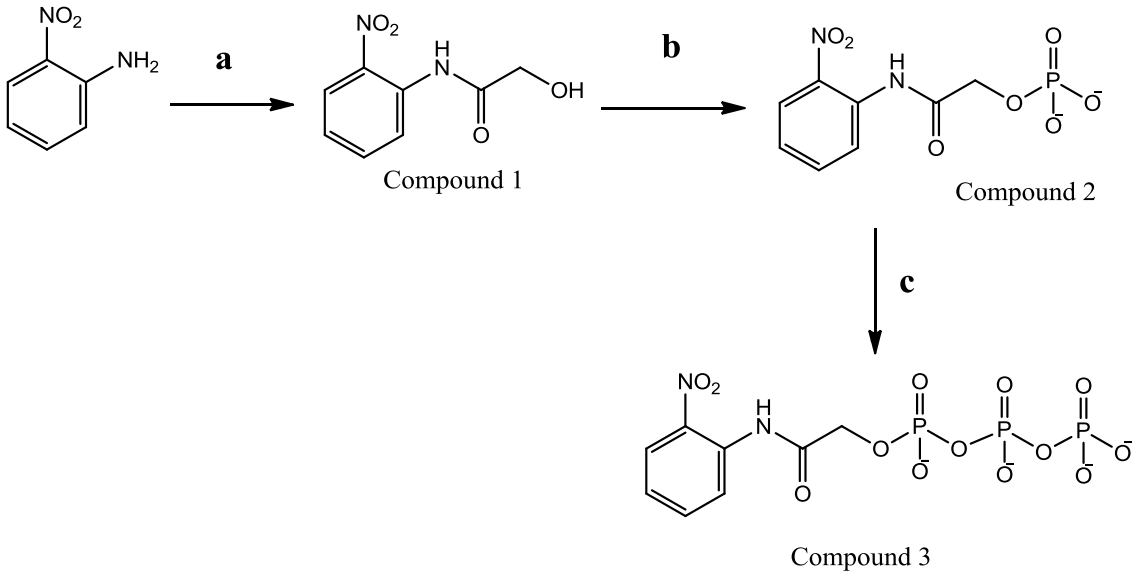

Synthetic scheme of NPhAdMTP: **a**) Ethyl glycolate, reflux, 170° C, 8 days. **b**) $POCl_3$, Triethylphosphate, NaOH, rt, overnight. **c**) Tributylamine, Carbonyldiimidazole, Pyrophosphate, dry DMF, Ar atmosphere, rt, overnight.

Compound 1

2-Nitroaniline (14.5 g, 105 mmol) and ethyl glycolate (9.5 ml, 100 mmol) was refluxed at 170° C. After 8 days continuous stirring, the reaction mixture was extracted to ethyl acetate against 2N HCl solution. The organic layer was evaporated and dried over $MgSO_4$. The residue was purified by silica gel column chromatography. (Dichloromethane/Ethyl acetate, 7:3) and obtained in 5.1% yield (1g). ^{1}H-NMR [$CDCl_3$ (TMS)]. δ= 2.96 (1H, s), 4.33 (2H, d, J= 9.3 Hz), 7.22 (1H, t, J= 7.9 Hz), 7.66 (1H, t, J=

7.8 Hz), 8.21 (1H, d, J= 8.5 Hz), 8.79 (1H, d, J= 8.6 Hz). ESI-MS: *m/z* = 196.12 [M+H^+] (calcd. 196.05).

Compound 2

A solution of $POCl_3$ (0.9 ml, 9.8 mmol) in triethylphosphate (5 ml) was placed in an ice bath and kept at 0° C under nitrogen condition. The solution was stirred vigorously while compound1 (0.59 g, 3.0 mmol) was added slowly in small quantities. The reaction was allowed to proceed for overnight at 0° C. Unreacted POCl3 was removed by rotary evaporation at 30° C. While the solution was stirred vigorously at 0° C, 7 ml of 4N NaOH was added dropwise to hydrolyze the acid chloride. Cold water (50 ml, 4° C) was added and the pH was adjusted to 7.5 with 6M NaOH. The solution was applied to a DEAE-Sephadex A-25 column (2.5x30 cm, 20g) and eluted with a linear 0 -1.0 M (total volume 1 litre) triethylammonium hydrogencarbonate gradient at 4°C. The major peak of compound 2 was eluted at 0.69 M- 0.75 M (10 ml/tube). The collected fractions were evaporated with ethanol several times to remove triethylammonium hydrogencarbonate. Yield 14% (0.12 g). ^{1}H-NMR [D_2O (TMS)]. δ= 4.58 (2H, d, J= 7.2 Hz), 7.17 (1H, t, J= 7.9 Hz), 7.62 (1H, t, J= 7.8 Hz), 8.16 (1H, d, J= 8.5 Hz), 8.76 (1H, d, J= 8.6 Hz). ESI-MS: *m/z* = 276.52 [M-H^+] (calcd. 275.02).

Compound 3

The triethylammonium salt of compound 2 (0.12 g, 0.44 mmol) is converted in to tributylammonium salt by addition of tributylamine (0.2 ml, 0.75 mmol) in dry methanol (1.3 ml). Triethylamine and methanol were removed by rotary evaporation. The obtained tributylammonium salt was dissolved in dry DMF (1 ml). While stirring, 1,1'-carbonyldiimidazole (0.18 g, 1.1 mmol) dissolved in 1.4 ml of dry DMF was added under argon condition and the reaction was allowed to proceed for 18 hrs at room temperature. Excess 1,1' -carbonyldiimidazole was destroyed by addition of dry methanol (0.05 ml) and stirred for 1 hr. This solution was added dropwise with mixing to tributylammonium salt of pyrophospahate [which was prepared from tetrasodium pyrophosphate, 0.53 g, 1.12 mmol, as mentioned in the **section 2.3.4**] dissolved in dry DMF (1.5 ml). After reacting overnight at room temperature, the reaction mixture above was cooled to 0°C in an ice bath. Cold water (2 ml, 4°C) was added with mixing and the pH was brought to 7.5 with 1 M NaOH. Then the reaction mixture was extracted against ether/water mixture and water part was evaporated with ethanol at 30°C and dried. The dried residue was dissolved in 0.2 M triethylammonium hydrogencarbonate solution and applied to a DEAE-Sephadex A-25 column(2.5x30 cm, 20g) and eluted with a

linear 0.2-1.0 M (total volume 0.8 litre) triethylammonium hydrogencarbonate gradient at 4°C. The major peak of compound 4 was eluted at 0.69 M- 0.77 M (10 ml/tube). The collected fractions were confirmed by ESI-mass and evaporated with ethanol several times to remove triethylammonium hydrogencarbonate. The obtained product is converted to the sodium salt using 1M NaI-acetone [see **section 2.3.5**]. Yield 12% (0.014 g). ^{1}H-NMR [D_2O (TMS)]. δ= 4.68 (2H, d, 7.7 Hz), 7.47 (1H, t, J= 7.9), 7.79 (1H, t, J= 7.9 Hz), 8.04 (1H, d, J= 8.3 Hz), 8.19 (1H, d, J= 8.5 Hz). ESI-MS: *m/z* = 434.89 [M-H^+] (calcd. 434.94).

2.3.3 Synthesis of *para*-AzoTP

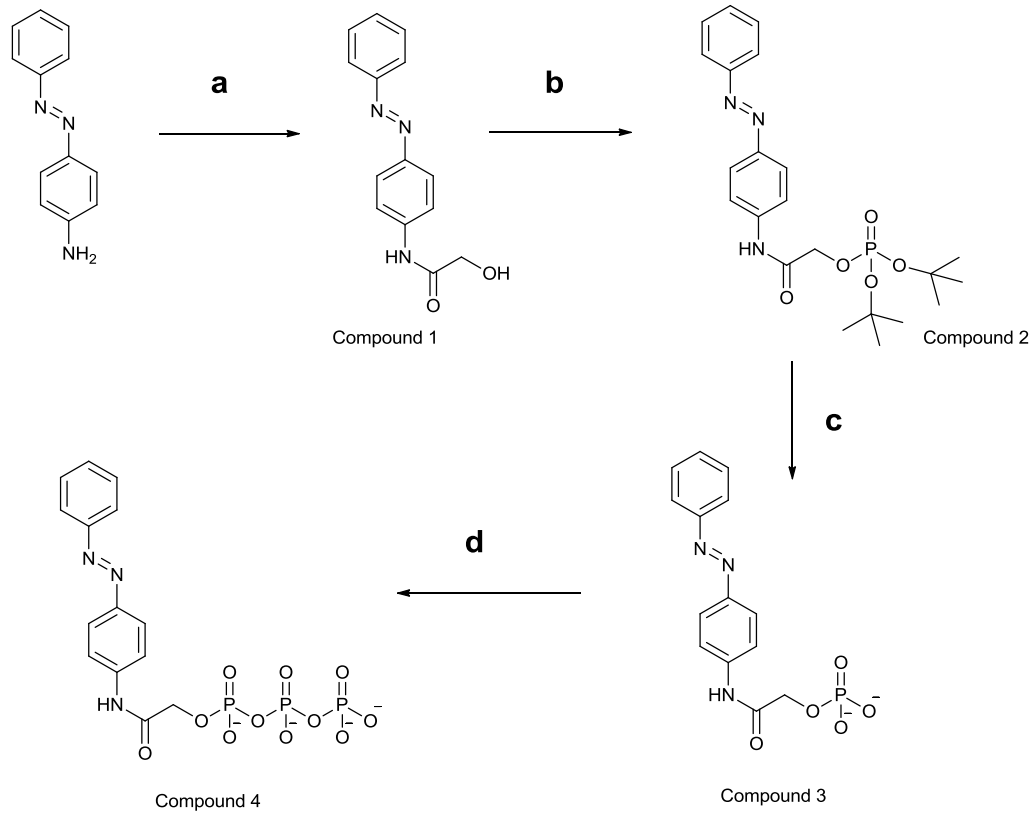

Synthetic scheme of *para*-AzoTP: **a**) $LiAlH_4$, Ethyl glycolate, dry THF, Ar atmosphere, rt, 18 hrs. **b**) di-*tert*-butyl N,N- diisopropylphosphoramidite, 1H-tetrazole, dry THF, Ar atmosphere, rt, 7 hrs. Then, mCPBA, 0°C, 1h and then rt, 40 min. **c**) Trifluoroacetic acid, dry CH_2Cl_2, Ar atmosphere, rt, 6 hrs. Then eluting through DEAE sephadex A-25 anion exchanger, TEAB. **d**) Tributylamine, Carbonyldiimidazole, Pyrophosphate, dry DMF, Ar atmosphere, rt, overnight.

Compound 1:

A solution of *p*-aminoazobenzene (6.0 g, 30.42 mmol) in dryTHF (5 ml) was added dropwise to a solution of lithium aluminium hydride (3 ml of 2 M solution in THF, 15 ml) with stirring at room temperature under argon atmosphere. After the addition, stirring was maintained for 30 minute. Then, ethyl glycolate (0.6 ml, 6.06 mmol) was added dropwise to the above mixture and kept for overnight stirring. Then reaction was quenched by successive addition of 0.4 ml of water, 0.4 ml of 10% NaOH, and 1.2 ml of water. The reaction mixture was then extracted against water/dichloromethane and organic layer was dried over $MgSO_4$ and concentrated in rotary evaporator. The residue was chromatographed on silica gel (ethyl acetate/dichloromethane, 1:1) and product obtained in 10% yield (0.8 g). ^{1}H-NMR [$CDCl_3$ (TMS)]- δ=2.48 (1H, t, J= 5.2 Hz), 4.30 (2H, d, J=5.2 Hz), 7.44-7.53 (3H, m), 7,75 (2H, d, J=8.8Hz), 7.92 (4H, dd, J=8.8, 7.2 Hz), 8.47 (1H, s).

Compound 2:

To a solution of compound 1 (1.02 g, 4 mmol) in 20 ml of dry THF and di-TERT-butyl N,N-diisopropylphosphoramidite (1.64 ml, 5.2mmol), 1H-Tetrasole (0.83 g, 12 mmol) was added and stirred for 7 hrs at room temperature. Then, a solution of 65% m-chloroperoxybenzoic acid (1.85 g, 6.93mmol) in 10 ml of dry dichloromethane was

added to above mixture and stirred for 1 h in an ice base, mixture again stirred for 25 min at room temperature and then saturated aqueous solution of $NaHCO_3$ (45 ml) was added and mixture was further stirred for 40 min. Then, ethyl acetate (130 ml) was added and resulting mixture washed with saturated aqueous solution of $NaHCO_3$ (twice) and NaCl (once) and then organic layer was dried over $MgSO_4$, evaporated and dried in vacuum. The compound was purified by silica gel column chromatography (Hexane/ Ethyl acetate, 2:8) and obtained in 24% yield (0.41 g).^{1}H-NMR[$CDCl_3$ (TMS)]-δ= 1.54 (18H, m), 4.54 (2H, d, J=8.8Hz), 7.47-7.51 (3H, m), 7.77 (2H, d, J=8.8Hz), 7.89-7.95 (4H, dd, J=8.4, 8.8Hz), 8.83 (1H, s).

Compound 3:

To a dry dichloromethane (5.4ml) solution of compound 2 (0.20 g, 0.46mmol), trifluoroacetic acid (0.56ml) was added, stirred for 3 hrs at room temperature and evaporated. After adding methanol (10ml), the mixture was evaporated and repeated the same more than some times to remove CF_3COOH completely and followed by washing with CH_2Cl_2. Removed all the solvents by rotary evaporator and dried in vacuum. To the residue, water was added and pH adjusted to 7.5 with 1M NaOH to obtain the clear solution. The dissolved product was converted to triethylammonium salt by eluting through a DEAE sephadex A-25 column with 0.5 M triethylammonium

hydrogencarbonate solution at 4˚C and eluted portion was evaporated with ethanol several times to remove triethyl ammonium hydrogencarbonate.. Yield= 85% (0.12g). ^{1}H-NMR [CD_3OD (TMS)]-δ= 4.57 (2H, d, J=8.4Hz), 7.47-7.54 (3H, m), 7.82 (2H, d, J=9.2Hz), 7.87-7.92 (4H, dd, J=6.8, 9.2Hz).

Compound 4:

The triethylammonium salt of compound 3 (0.24 g, 0.74mmol) is converted in to tirbutylammonium salt by addition of tributylamine (0.37 ml, 1.48 mmol) in dry methanol (2.6 ml). Triethylamine and methanol were removed by rotary evaporation. The obtained tributylammonium salt was dissolved in dry DMF (4.4 ml). While stirring, 1,1'-carbonyldiimidazole (0.44 g, 2.75 mmol) dissolved in 10 ml of dry DMF was added under argon condition and the reaction was allowed to proceed for 16 hrs at room temperature. Excess 1,1'-carbonyldiimidazole was destroyed by addition of dry methanol (0.1ml, 2mmol) and stirred for 1 hr. This solution was added dropwise with mixing to tributylammonium salt of pyrophospahate [which was prepared from tetrasodium pyrophosphate, (1.30 g, 2.79mmol), as mentioned in the **section 2.3.4**] dissolved in dry DMF (3.7 ml). After reacting overnight at room temperature, the reaction mixture above was cooled to 0℃ in an ice bath. Cold water (5ml, 4℃) was added with mixing and the pH was brought to 7.5 with 1M NaOH. Then the reaction

mixture was extracted against ether/water mixture and water part was evaporated with ethanol at 30℃ and dried. The dried residue was dissolved in 0.2M triethylammonium hydrogencarbonete solution and applied to a DEAE-Sephadex A-25 column (2.5×30 cm, 20 g) and eluted with a liner 0.2-1.0M (total volume 1 liter) triethylammonium hydrogen carbonate gradient at 4℃. The major peak of compound 4 was eluted at 1.0M (10ml/tube). The collected fractions were confirmed by ESI-mass and evaporated with ethanol several times to remove triethylammonium hydrogencarbonate. The obtained product is converted to the sodium salt using 1M NaI-acetone [see **section 2.3.5**]. Product purity was evaluated by thin layer chromatography, using silica gel 60RP-18 $F_{254}S$ and methanol/water (1:1) mobile phase. Yield= 23% (0.1g). ^{1}H-NMR [D_2O (TMS)]-δ= 4.66 (2H, d, J= 7.2), 7.62 (3H, m), 7.76 (2H, d, J= 9.2), 7.85 (4H, dd, J= 6.8, 8.8).

2.3.4 Synthesis of AzoTP.

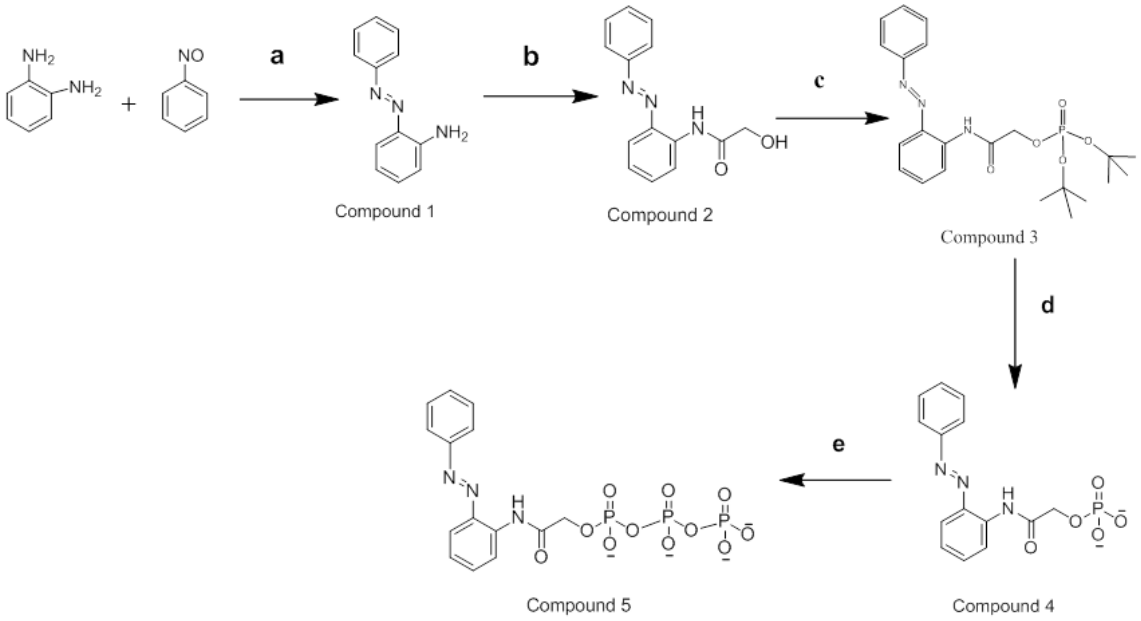

Synthetic scheme of AzoTP: **a**) AcOH, Toluene, N_2 atmosphere, 60°C, 20 hrs. b) $LiAlH_4$, Ethyl glycolate, dry THF, Ar atmosphere, rt, 18 hrs. **c**) di-*tert*-butyl N,N-diisopropylphosphoramidite, 1H-tetrazole, dry THF, Ar atmosphere, rt, 7 hrs. Then, mCPBA, 0°C, 1h and then rt, 40 min. **d**) Trifluoroacetic acid, dry CH_2Cl_2, Ar atmosphere, rt, 6 hrs. Then eluting through DEAE sephadex A-25 anion exchanger, TEAB. **e**) Tributylamine, Carbonyldiimidazole, Pyrophosphate, dry DMF, Ar atmosphere, rt, overnight.

Compound 1:

A solution of 1,2-phenylenediamine (8.2 g, 75.8 mmol) in toluene (500 ml) was degassed with a nitrogen stream for 20 min. Then, nitrosobenzene (8.12 g, 75.8 mmol) and acetic acid (4 equiv.) were added under nitrogen condition. The mixture was stirred at 60˚C for 24 h and the solvent was removed under reduced pressure. The residue was extracted with water/dichloromethane mixture. The organic portion is dried ($MgSO_4$) and evaporated in a rotary evaporator. The resultant residue was purified by silica gel column chromatography (Hexane/Ethyl acetate, 8:2) and product obtained in 42% yield (6.3 g). ^{1}H-NMR [$CDCl_3$ (TMS)]- δ= 5.9 (2H, br), 6.77 (1H, d, *J*=8.2 Hz), 6.82 (1H, dd, *J*=7.6, 7.6 Hz), 7.21 (1H, dd, *J*= 7.6. 7.7 Hz), 7.41 (1H, t, *J*= 7.3 Hz), 7.49 (2H, dd, *J*=7.2, 7.7 Hz), 7.82-7.85 (3H,m). ESI-MS: *m/z* = 198.12 [$M+H^+$] (calcd. 198.1).

Compound 2:

A solution of compound 1 (5.91 g, 30 mmol) in dryTHF (2 ml) was added dropwise to a solution of lithium aluminium hydride (3 ml of 2M solution in THF, 6 mmol) with stirring at room temperature under nitrogen atmosphere. After the addition, stirring was maintained for 40 minutes. Then, ethyl glycolate (0.57 ml, 6 mmol) was added dropwise to the above mixture and kept for overnight stirring. Then reaction was carefully quenched by successive addition of water (0.3 ml), 10% NaOH (0.3 ml) and again water

(1 ml). The reaction mixture was then extracted against water/dichloromethane and dichloromethane part dried over MgSO4 and concentrated in rotary evaporator. The residue was chromatographed on silica gel (Hexane/ Ethyl acetate, 6:4) and product obtained in 22% yield (1.68 g). ^{1}H-NMR [$CDCl_3$ (TMS)]- δ= 2.46 (1H, t, *J*= 5.4 Hz), 4.35 (2H, d, *J*= 5.4 Hz), 7.21 (1H, dd, *J*= 7.6, 7.8 Hz), 7.47-7.56 (4H, m), 7.89 (1H, d, *J*= 8 Hz), 7.92 (2H, d, *J*=8.4 Hz), 8.72 (1H, d, *J*=8.4 Hz), 11.0 (1H, br). ESI-MS: *m/z* = 278.12 [$M+Na^+$] (calcd. 278.09).

Compound 3:

To a solution of compound 2 (1.02 g, 4 mmol) in 20 ml of dry THF and di-*tert*-butyl *N*,*N*-diisopropylphosphoramidite (1.64 ml, 5.2 mmol), 1H-Tetrazole (0.83 g, 12 mmol) was added and stirred for 7 hrs at room temperature. Then, a solution of 65% *m*-chloroperoxybenzoic acid (1.85 g、6.93 mmol) in 10 ml of dry dichloromethane was added to the above mixture and stirred for 1 h in an ice bath. After taking from ice bath, mixture again stirred for 25 min at room temperature and then saturated aqueous solution of NaHCO3 (45 ml) was added and mixture was further stirred for 40 min. Then, ethyl acetate (130 ml) was added and resulting mixture washed with saturated aqueous solutions of NaHCO3 (twice) and NaCl (once) and then organic layer was dried over MgSO4 , evaporated and dried in vacuum. The compound was purified by

silica gel column chromatography (Hexane/ Ethyl acetate, 6:4) and obtained in 38 % yield (0.68 g). ^{1}H-NMR [$CDCl_3$ (TMS)]- δ= 1.46 (18H, s), 4.60 (2H, d, *J*=7.1 Hz), 7.21 (1H, dd, *J*= 7.7, 7.8 Hz), 7.47-7.52 (2H, m), 7.56 (2H, dd, *J*= 7.2, 8 Hz), 7.88 (1H, d, *J*= 8 Hz), 8.05 (2H, d, *J*=8.5 Hz), 8.70(1H, d, *J*=8.4 Hz), 10.73 (1H, br). ESI-MS: *m/z* = 448.22 [$M+H^+$] (calcd. 448.20).

Compound 4:

To a dry dichloromethane (16 ml) solution of compound 3 (0.65 g, 1.45 mmol), trifluoroacetic acid (1.77 ml) was added, stirred for 6 hrs at room temperature and evaporated. After adding methanol (30 ml), the mixture was evaporated and repeated the same more than three times to remove CF_3COOH completely and followed by washing with CH_2Cl_2. Removed all the solvents by rotary evaporator and dried in vacuum. To the residue, water was added and pH adjusted to 7.5 with 1M NaOH to obtain the clear solution. The dissolved product was converted to triethylammonium salt by eluting through a DEAE sephadex A-25 column with 0.5 M triethylammonium hydrogencarbonate solution at 4˚C and eluted portion was evaporated with ethanol several times to remove triethyl ammonium hydrogencarbonate. Yield= 95 % (0.73 g). ^{1}H-NMR [CD_3OD (TMS)]- δ= 4.62 (2H, d, *J*= 6.6 Hz), 7.25 (1H, dd, *J*= 7.7, 7.8 Hz), 7.50-7.59 (4H, m), 7.89 (1H, d, *J*= 8.2 Hz), 8.07 (2H, d, *J*= 8.5 Hz), 8.63 (1H, d, *J*=8.4

Hz). ESI-MS: *m/z* = 334.06 [M-H^+] (calcd. 334.06).

Compound 5:

The triethylammonium salt of compound 4 (0.64 g, 1.2 mmol) is converted in to tributylammonium salt by addition of tributylamine (1 ml, 4 mmol) in dry methanol (7 ml). Triethylamine and methanol were removed by rotary evaporation. The obtained tributylammonium salt was dissolved in dry DMF (12 ml). While stirring, 1,1'-carbonyldiimidazole (1.2 g, 7.5 mmol) dissolved in 10 ml of dry DMF was added under argon condition and the reaction was allowed to proceed for 16 hrs at room temperature. Excess 1,1'-carbonyldiimidazole was destroyed by addition of dry methanol (6 mmol, 0.3 ml) and stirred for 1 hr. This solution was added dropwise with mixing to tributylammonium salt of pyrophospahate [which was prepared from tetrasodium pyrophosphate, 3.5 g, 7.5 mmol, as mentioned in the **section 2.3.4**] dissolved in dry DMF (10 ml). After reacting overnight at room temperature, the reaction mixture above was cooled to 0°C in an ice bath. Cold water (15 ml, 4°C) was added with mixing and the pH was brought to 7.5 with 1 M NaOH. Then the reaction mixture was extracted against ether/water mixture and water part was evaporated with ethanol at 30°C and dried. The dried residue was dissolved in 0.2 M triethylammonium hydrogencarbonate solution and applied to a DEAE-Sephadex A-25 column(2.5x30 cm,

20g) and eluted with a linear 0.2-1.0 M (total volume 1 litre) triethylammonium hydrogencarbonate gradient at 4°C. The major peak of compound 5 was eluted at 0.67 M- 0.86 M (10 ml/tube). The collected fractions were confirmed by ESI-mass and evaporated with ethanol several times to remove triethylammonium hydrogencarbonate. The obtained product is converted to the sodium salt using 1M NaI-acetone [see **section 2.3.5**]. Product purity was evaluated by thin layer chromatography, using silica gel 60 RP-18 $F_{254}S$ and acetonitrile/water (2:8) mobile phase. Yield= 71 % (0.5 g). ^{1}H-NMR [D_2O (TMS)]- δ= 4.71 (2H, d, *J*=7.4 Hz), 7.45 (1H, dd, *J*= 7.7, 7.8 Hz), 7.61-7.68 (4H, m), 7.76 (1H, d, *J*= 8 Hz), 7.97-8.02 (3H, m). ^{13}C-NMRδ= 170.80, 170.70, 152.71, 143.51, 134.66, 133.26, 132.74, 130.29, 127.23, 124.33, 123.56, 117.73, 65.41. (Here, the peaks at 170.80 and 170.70 most probably explained by carbonyl carbons in the amide group of two possible isomers by the *cis-trans* orientations around C-N bond). ESI-MS: *m/z* = 494.00 [M-H^+] (calcd. 494.00).

2.3.5 Preparation of Tributylammonium pyrophosphate

A solution of tetrasodium pyrophosphate (3.5 g, 7.5 mmol) in 50 ml water was eluted through a cation exchange resin (BIO-RAD AG 50 W-X8 Resin, 50-100 mesh, hydrogen form) at 4°C. The eluent with pH below 3 (pH paper) was collected directly into vigorously stirred tributylamine (2 ml, 8 mmol, 4°C). The obtained tributylammonium pyrophosphate was dried by repeated rotary evaporation with dry methanol and then dissolved in dry DMF (10 ml).

2.3.6 Conversion of triethylammonium salt of triphosphate to sodium salt:

The solid triethylammonium salt of compound 5 (~ 0.6 g) was dissolved in 2 ml of dry methanol. The sodium salt of the product was precipitated as the sodium salts by the addition of NaI-acetone solution (20 ml, 1M) and washed several times with acetone. The residue was freeze-dried and stored at -18°C.

2.3.7 ESI-MASS Spectra of AzoTP:

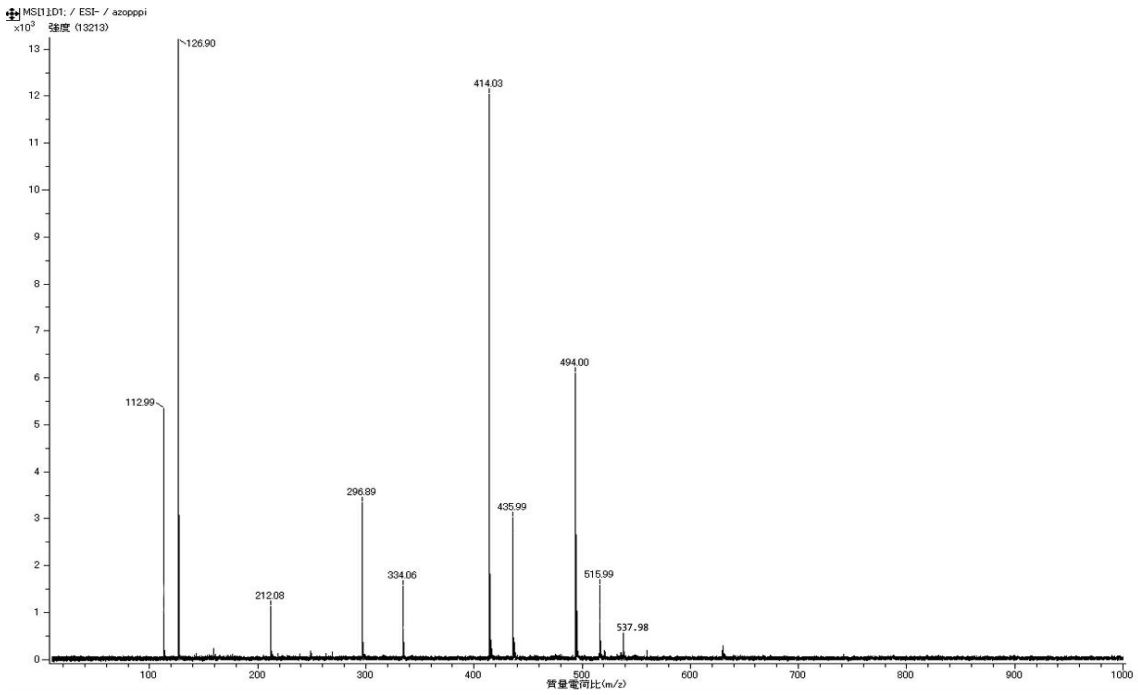

Figure 1. The peaks at 537.98, 515.99 and 494.00 can be assigned to [M-H^+] of disodium, monosodium and tetra-protonated AzoTPs respectively. The peaks at 435.99, 414.03 and 334.06 are the fragment peaks of AzoTP with the structure of NaAzoTP – P_i, AzoTP – P_i and AzoTP – $2P_i$ respectively. The fragments at 296.89, 212.08, 126.90 and 112.99 are not assigned.

2.3.8 Absorption Spectra of AzoTP:

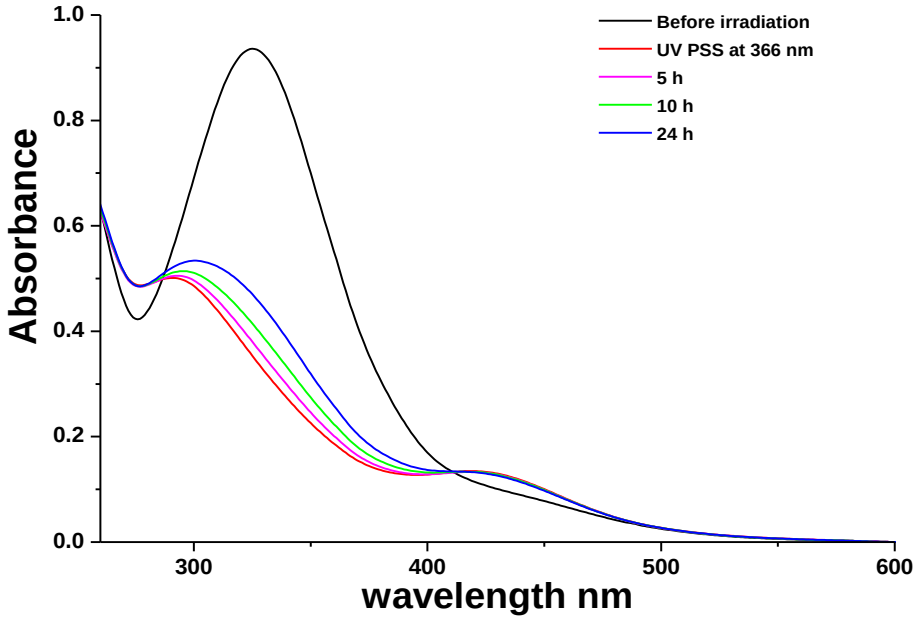

Figure 2. Absorption spectral change of AzoTP in BRB80 buffer with incubation time in the dark at 23°C after 20 s irradiation at 366 nm. The measured molar extinction coefficient for the *trans* AzoTP was 16044 M^{-1} cm^{-1} at 327 nm.

2.3.9 HPLC profile of AzoTP:

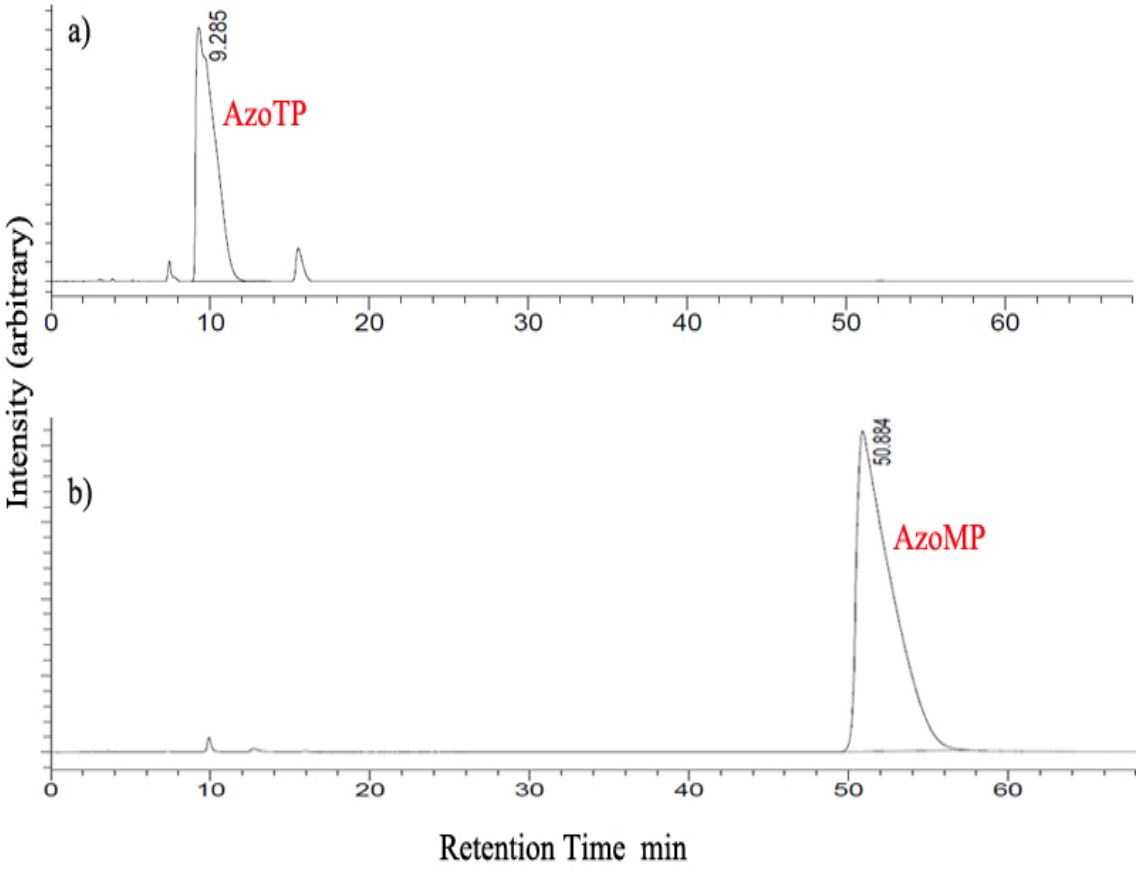

Figure 3. Reverse-phase HPLC profile of AzoTP. Chromatograms of, (**a**) Azo-triphosphate (AzoTP), (b) Azo-monophosphate (AzoMP) in water. Conditions of the RP-HPLC analysis; Column: CN-80Ts, 4.6x250 mm (TOSOH). Eluent: 20% of CH_3CN in aqueous solution of 0.1 M NaH_2PO_4. Monitoring wavelength: λ= 327 nm. Flow rate: 1.0 mL/min at room temperature (23°C). Injection volume: 50 µL.

2.4 Kinesin-microtubule motility system.

2.4.1 Flow cell:

The two strips of double-sided adhesive tape were placed on a glass slide, ca. 2 mm apart, and covered with a cover slip (18x18 mm) providing a flow cell with working volume 3-5 μL. The solutions were pipetted on one side and withdrawn from the other through capillary action, using a Whatman filter paper or a Kimwipe, as described previously.

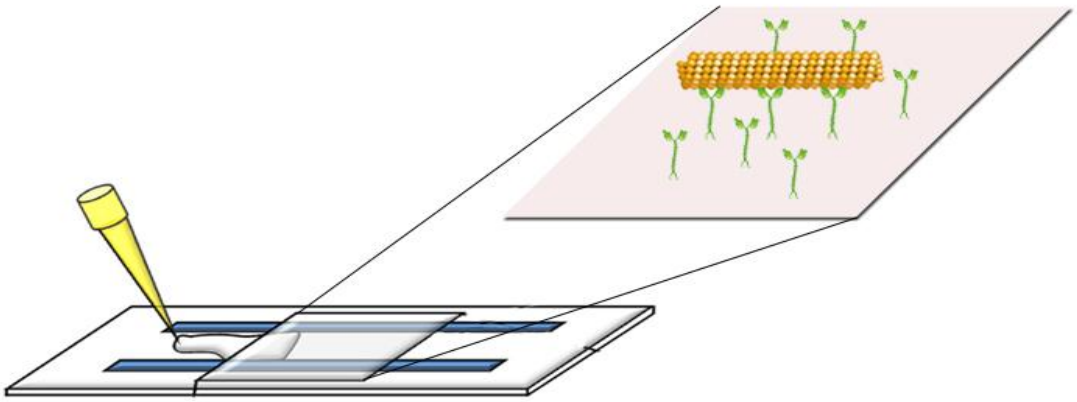

Figure 1. The schematic representation of flow cell (interior volume ~ 3-5 μL) for the kinesin-microtubule motility assay.

2.4.2 Protein purifications and preparations:

Tubulins were purified from porcin brains through two cycles of polymerization-depolymerization processes in the presence of a high-molarity PIPES buffer. Microtubules were polymerized using the purified tubulins and labeled with CF™ 633 succinimidyl ester. Kinesin utilized in this research was a recombinant kinesin consist of 573 amino acid residues from N-terminus of a conventional human kinesin. This recombinant kinesin fused with His-tag in the N-terminus (plasmid: pET 30b) was expressed in *E. coli* Rossetta (DE3)pLysS and purified by the general method utilizing Ni-NTA-agarose.

2.4.3 Buffers:

Kinesin buffer

80 mM PIPES (pH 7.5) + 1mM EGTA + 2 mM $MgSO_4$ + 0.5 mg/mL casein.

Microtubule buffer:

80 mM PIPES (pH 7.5) + 1mM EGTA + 2 mM $MgSO_4$ + 10 µM taxol + 0.1 mg/mL casein.

Assay buffer

80 mM PIPES (pH 7.5) + 1mM EGTA + 2 mM $MgSO_4$ + 0.5 mg/mL casein + 10 µM taxol + Anti-fade reagents [0.14M β-mercaptoethanol + 20mM glucose + 20 µg/mL catalase + 0.1 mg/mL glucose oxidase] + AzoTP.

2.4.4 Procedure:

The kinesin solution 3 µL (diluted with kinesin buffer, ca. 100µg/mL) was perfused to flow cell and incubated for 3 min. Then the microtubule solution 3µL (diluted with microtubule buffer, ca. 0.5µM) was perfused into the flow cell and incubated for 3 min. The flow cell was rinsed with 3 µL of microtubule buffer to remove unbound microtubules. After 1 min incubation, 3 µL of motility buffer with desired concentration of AzoTP was perfused into the flow cell and the motility of microtubules was monitored and recorded using fluorescence microscope. The flow cell that had been irradiated with UV (10 seconds) or visible light (30 seconds) was analyzed to determine the gliding motility each time.

2.5 Actomyosin motility system.

2.5.1 Flow cells:

The two strips of double-sided adhesive tape were placed on a glass slide, ca. 5 mm apart, and covered with a 18x18 mm cover slip (coated with 0.01% of nitrocellulose in amyl acetate and dried on a hot plate at 80°C for 2-3 minutes) providing a flow cell with working volume 15 μL. The solutions were pipetted on one side and withdrawn from the other through capillary action, using a Whatman filter paper.

2.5.2 Buffers:

DTT-assay buffer

100 mM HEPES (pH 7.4) + 25 mM NaCl + 4 mM $MgCl_2$ + 1 mM EGTA + 10 mM DTT.

BSA-DTT-assay buffer

100 mM HEPES (pH 7.4) + 25 mM NaCl + 4 mM $MgCl_2$ + 1 mM EGTA + 0.5 mg/mL BSA + 10 mM DTT.

ATP/AzoTP-assay buffer

100 mM HEPES (pH 7.4) + 25 mM NaCl + 4 mM $MgCl_2$ + 1 mM EGTA + 0.5 mg/mL BSA + 10 mM DTT + 20mM glucose + 20 µg/mL catalase + 0.1 mg/mL glucose oxidase + ATP/AzoTP.

2.5.3 Procedure:

The myosin solution 15 µL (diluted with DTT-assay buffer, ca. 0.29 mg/mL) was perfused two times (total 30 µL) to flow cell and incubated for 2 minutes. Then flow cell was washed with 2x15 µL of BSA-DTT-assay buffer and actin solution 2x15 µL (diluted with BSA-DTT-assay buffer, ca. 20 µg/mL) was perfused. After 2 minutes incubation, the flow cell was washed with 2x15 µL of BSA-DTT-assay buffer. Then 2x15 µL of ATP/AzoTP-assay buffer was perfused into the flow cell and the motility of actin filaments were monitored and recorded using fluorescence microscope.

2.6 F_1-ATPase rotation and hydrolysis assay system:

2.6.1 Measurement of hydrolysis activity.

a) Buffers:

Assay buffer

50 mM HEPES/KOH (pH 8.0) + 100 mM KCl + x mM ATP or AzoTP

+ x mM $MgCl_2$ (here, x = desired concentration)

Protein buffer

50 mM HEPES/KOH (pH 8.0) + 100 mM KCl + 100-150 nM F_1- ATPase for AzoTP. (10 nM F_1-ATPase for ATP).

b) Calibration curve:

The standard calibration curve was prepared by 1M potassium phosphate solution.

c) Procedure:

- Add 5 µL of protein buffer into 45µL of assay buffer.
- Incubation at 25° C for 1 hour.
- Add 100 µL of 8% Trichloroacetic acid (TCA) to stop the reaction.
- Add 100 µL of ammonium molybdate buffer and incubate at room

temperature for 20 minutes.

- Add 100 μL of hydrazine sulfate buffer and incubate at room temperature for 20 minutes.
- Measure the absorbance at 630 nm.

2.6.2 Single molecule rotation assay of F1-ATPase:

a) Buffer:

Assay buffer

50 mM HEPES/KOH (pH 8.0) + 100 mM KCl + x mM ATP or AzoTP + x mM $MgCl_2$ + 2 mM PEP + 100 μg/mL PK. (here, x = desired concentration).

Buffer A

20 M potassium phosphate (pH 7.0) + 100 mM KCl + 0.5% BSA

Buffer B

50 mM HEPES/KOH (pH 8.0) + 100 mM KCl

b) Flow chamber:

Two pieces of backing papers of thin Parafilm were placed on a glass slide and covered with a cover slip providing enough space to immobilize the motor protein.

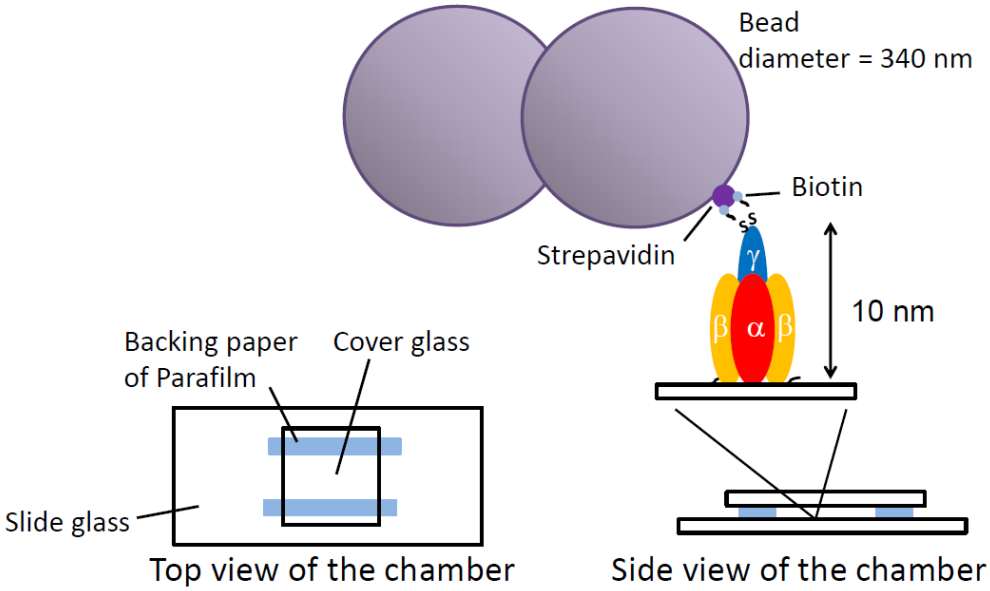

Figure 2. The flow chamber for the single molecular observation of F_1-ATPase.

c) <u>Procedure:</u>

- The enzyme solution (15 µL) perfused into the chamber and incubated at room temperature for 2 minutes.
- Then, chamber was washed with buffer A (50 µL).
- Bead solution (15 µL, diluted in buffer A) was perfused and incubated at room temperature for 15 minutes.
- Wash with buffer B (50 µL)
- Then, assay buffer (50 µL) was perfused and started the single molecular observation.

3. Results and discussion:

3.1 Kinesin-microtubule motility assay.

Kinesin[2] is a microtubule-based motor protein that plays substantial roles in many cellular processes in eukaryotic cells. The kinesin motor transports various cargos along microtubule filaments, employing adenosine triphosphate (ATP) as its energy source.[16–18] The kinesin-microtubule motility system is an exquisite model of biologically derived nanoscale motion. Among the several nucleosides and other ATP analogues have been applied to study the motile activities of kinesin motor protein,[19–21] multifunctional species have been particularly useful for *in vitro* kinetic studies of biological motor proteins.[20,21] Azobenzene is one of the most studied photochromic compounds[22] because it undergoes *cis*-to-*trans* photoisomerization that can be switched at particular wavelengths of light. The photoinduced isomerization of azobenzene moieties has been applied to the switching functions of various biomolecules.[23] It remains a challenge, however, to control the motile activities of kinesin motor protein reversibly through the photoisomerization of azobenzene.[14] Recently, our group synthesized ATP analogues substituted with an azobenzene unit at the ribose group and used them to drive and reversibly photocontrol the

kinesin-microtubule motility system;[15] the observed change in the motility upon photoirradiation of the ATP analogue was, however, far from satisfactory.

In this present study, we used a novel photoresponsive non-nucleoside triphosphate as a substrate to drive microtubule gliding on a kinesin-coated glass surface and to regulate its motility reversibly through alternating irradiation at two different wavelengths.[24]

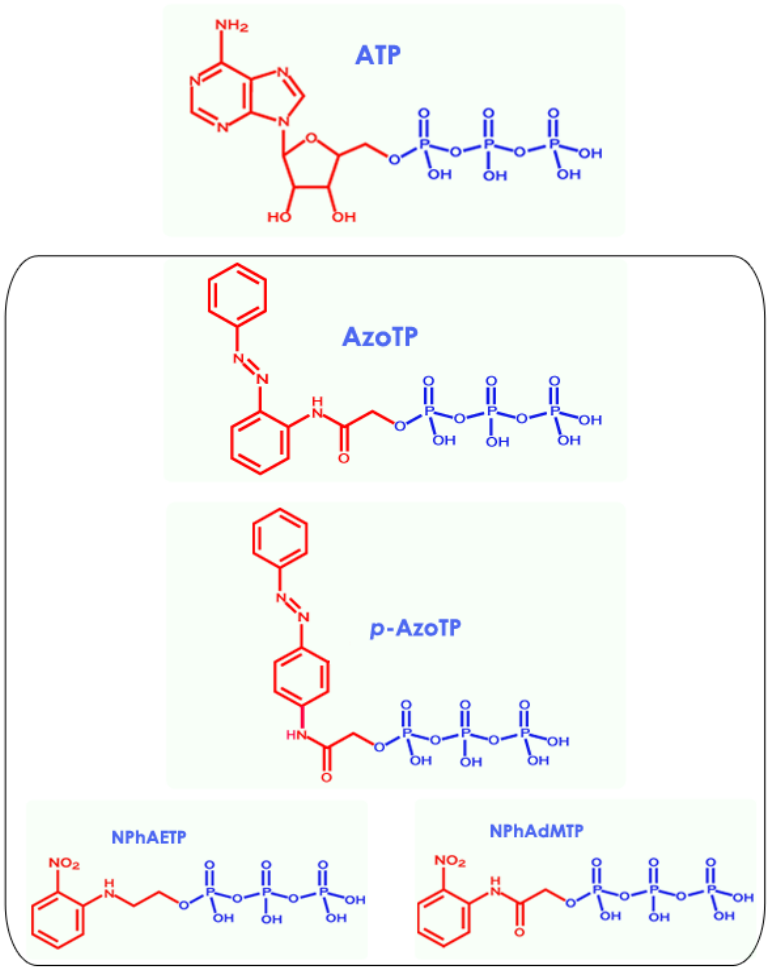

Figure 1. Structures of adenosine triphosphate (ATP) and the non-nucleoside triphosphates AzoTP, *p*-AzoTP, NPhAETP and NPhAdMTP.

NPhAETP (**Figure 1**) has been reported as a substrate for the actomyosin motor protein system.[25] Here, we synthesized NPhAdMTP (**Figure 1**) as a new amide version of NPhAETP to investigate the effect of the linkage between the aromatic ring and the triphosphate; we also synthesized AzoTP by exchanging the nitro group of NPhAdMTP with a photoresponsive phenylazo group. *p*-AzoTP synthesized in such a way that amide-triphosphate part incorporated to the *para* position of azobenzene (**Figure 1**). We characterized these compounds using ^{1}H NMR spectroscopy and electrospray ionization (ESI) mass spectrometry.

With these compounds in hand, we performed an *in vitro* microtubule gliding assay[26] using the flow cell method. In this assay, we employed fluorescence optical microscopy to visualize the gliding motility of fluorescently labeled microtubules[27] on a kinesin-coated glass surface. We calculated the gliding velocity by tracing the leading point of microtubules over a period of 40 s.

The motility experiments revealed that all four of the tested compounds—NPhAETP, NPhAdMTP, AzoTP and *p*-AzoTP —are capable of driving microtubule motility. NPhAETP and NPhAdMTP provided saturated gliding velocities for the microtubules of only 0.03 and 0.04 μm/s, respectively; these values are 4 and 6%, respectively, of the saturated velocity driven by 1 mM of ATP (0.67 μm/s). In case of

kinesin, NPhAETP functioned, but with limited efficiency compared with that of myosin. Our results suggested that changing the linkage between the aromatic ring and triphosphate unit from an amino to an amido group did not affect the activity significantly. In contrast to the performance induced by these two nitro derivatives, AzoTP provided high microtubule gliding motility (0.33 μm/s) at a concentration of 3 mM,[28] corresponding to 49% of the velocity of the motility driven by 1 mM ATP. But, *p*-AzoTP shows low gliding velocity of microtubules of only 0.05 μm/s at a concentration of 3 mM, corresponding to 7% of the motility driven by 1 mM ATP. These results indicate that both the structure of the aromatic group and position of the triphosphate moiety on the aromatic group have significant effect on the activity when used as a substrate of kinesin.

Figure 2 displays the changes in the absorption spectra of an aqueous solution of AzoTP upon irradiation with UV and visible light. Under irradiation at 366 nm, the AzoTP solution reached a *cis*-rich photostationary state (PSS); subsequent irradiation at 436 nm led to *cis*-to-*trans* conversion and re-establishment of the *trans*-rich PSS. Accordingly, we examined the effect of the photoinduced isomerization of AzoTP on the microtubule gliding velocity. **Figure 3** represents fluorescence images of gliding microtubules after 0 and 20 s for both the non-irradiated state and the 366-nm PSS in

the same flow cell.

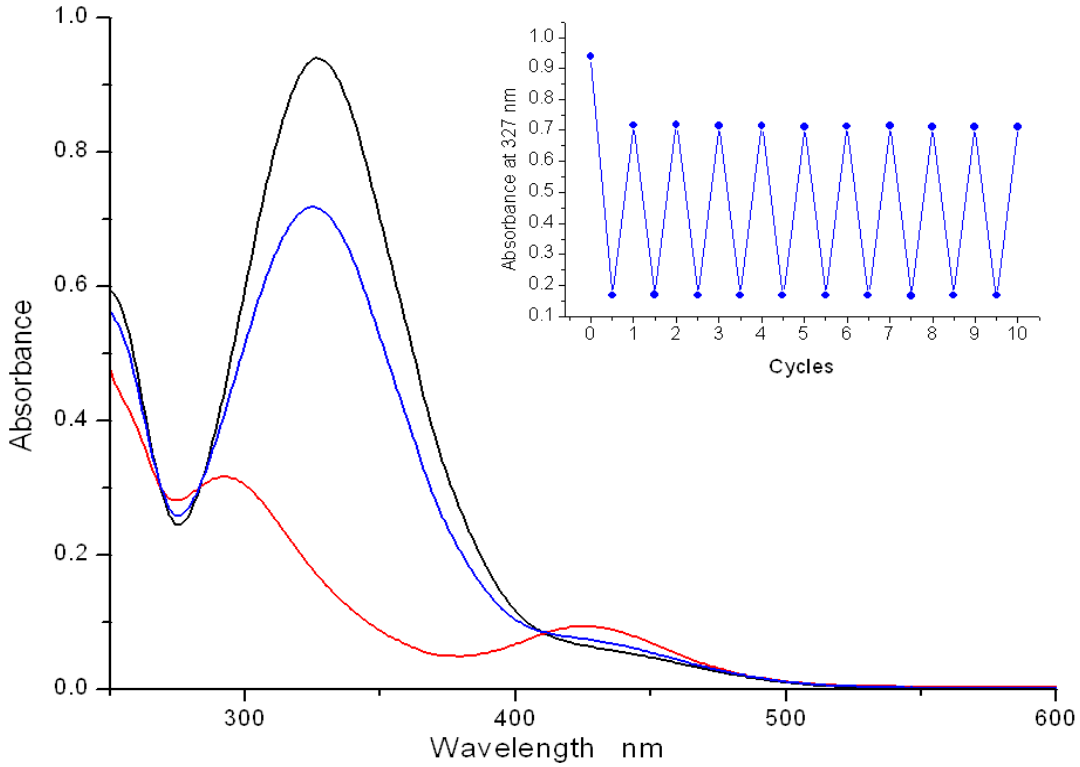

Figure 2. UV-vis absorption spectra of AzoTP (5.85 x 10^{-5} M) in water. (Black line) Before irradiation. (Red line) Photostationary state (PSS) at 366 nm. (Blue line) PSS at 436 nm. Inset: Absorbance changes at 327 nm after the alternative irradiation at 366 nm and 436 nm upto 10 cycles.

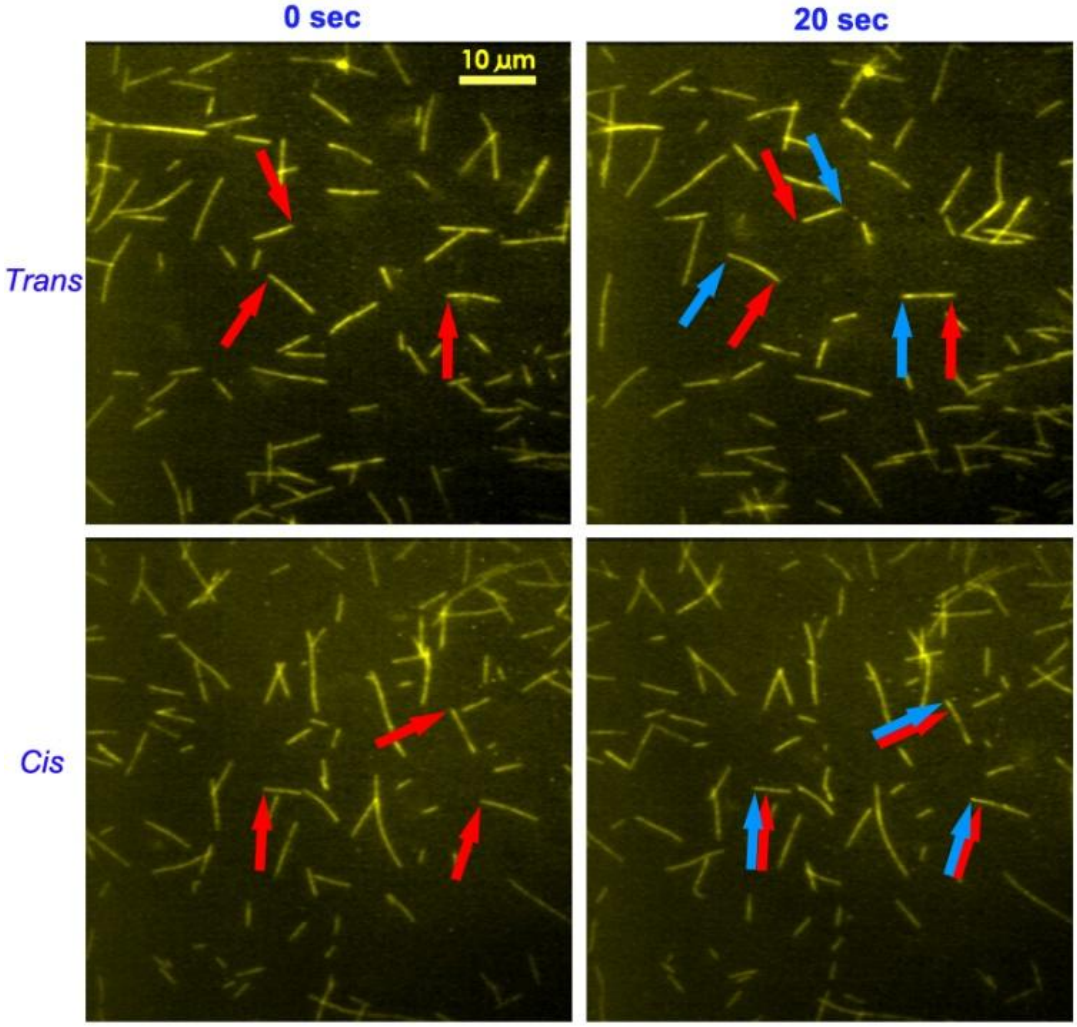

Figure 3 Fluorescence images of the gliding microtubules driven by AzoTP (3 mM) on the kinesin-adsorbed glass surface. (Top) Non-irradiated state at 0 s (left) and 20 s (right), and (bottom) 366 nm irradiated state at 0 s and 20 s in the flow cell. Red arrows indicate the leading points of microtubules at 0 sec and blue arrows indicate the leading points of the same microtubules at 20 sec.

Direct UV irradiation of the flow cell converted *trans*-AzoTP to its *cis* form, thereby decreasing the gliding velocity of the microtubules from 0.33 to 0.07 μm/s. Subsequent irradiation with visible light led to recovery of the initial velocity of the microtubule (to 0.28 μm/s), due to *cis*-to-*trans* isomerization of AzoTP.

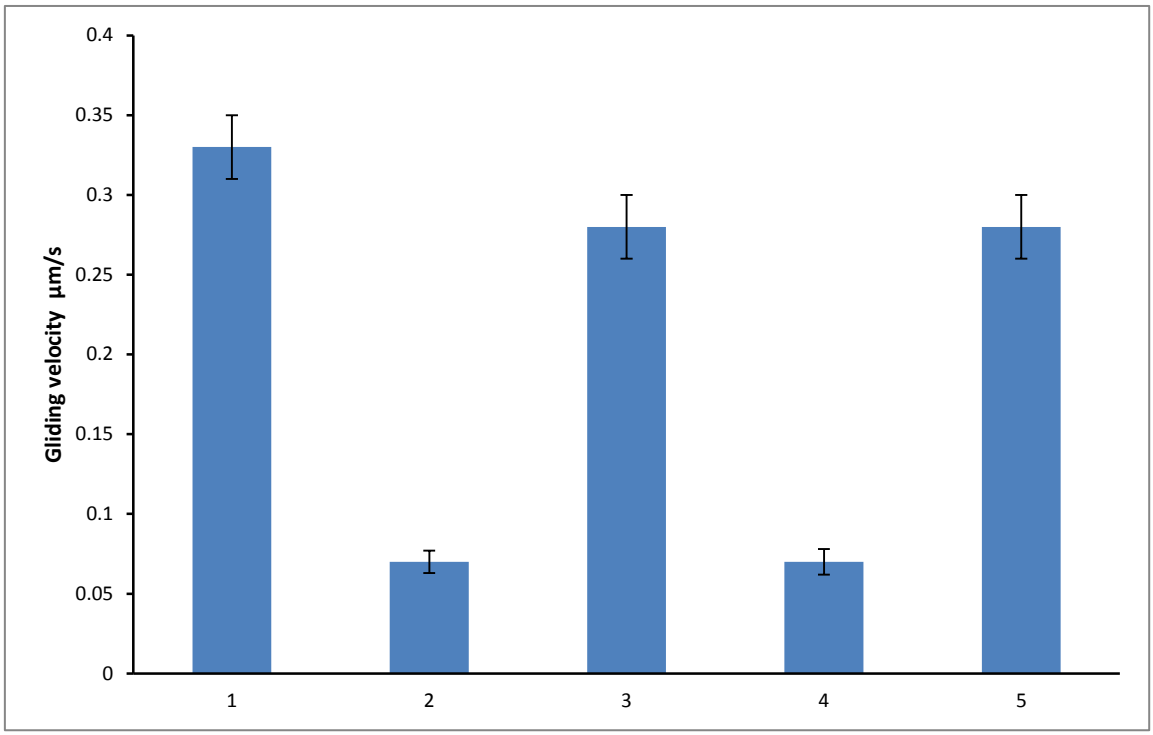

Figure 4 Repeatable changes in the gliding velocity of microtubules in the presence of AzoTP (3 mM) by the alternative UV and visible light irradiations. 1) Before irradiation. 2) After UV (366nm) irradiation for 10 s. 3) After subsequent irradiation at 436 nm for 30 s. 4) After subsequent UV irradiation for 10 s. 5) After subsequent irradiation at 436 nm for 30 s. Error bars represent standard deviations for 10 microtubules.

Figure 4 displays the changes in motility over two cycles of alternating irradiation with UV and visible light. The maximum decrease in velocity after photoirradiation of 3 mM AzoTP was 79% of the initial velocity of the *trans* form. The photocontrol over the changes in velocity between the *cis*-rich and *trans* states was repeatable for up to 10 cycles of irradiation with UV and visible light (**Figure 5**). To test the effect of the irradiation on the motility of the microtubules, we performed a control experiment using 1 mM ATP; we observed no significant changes in motility upon alternating irradiation with UV and visible light (**Figure 6**).

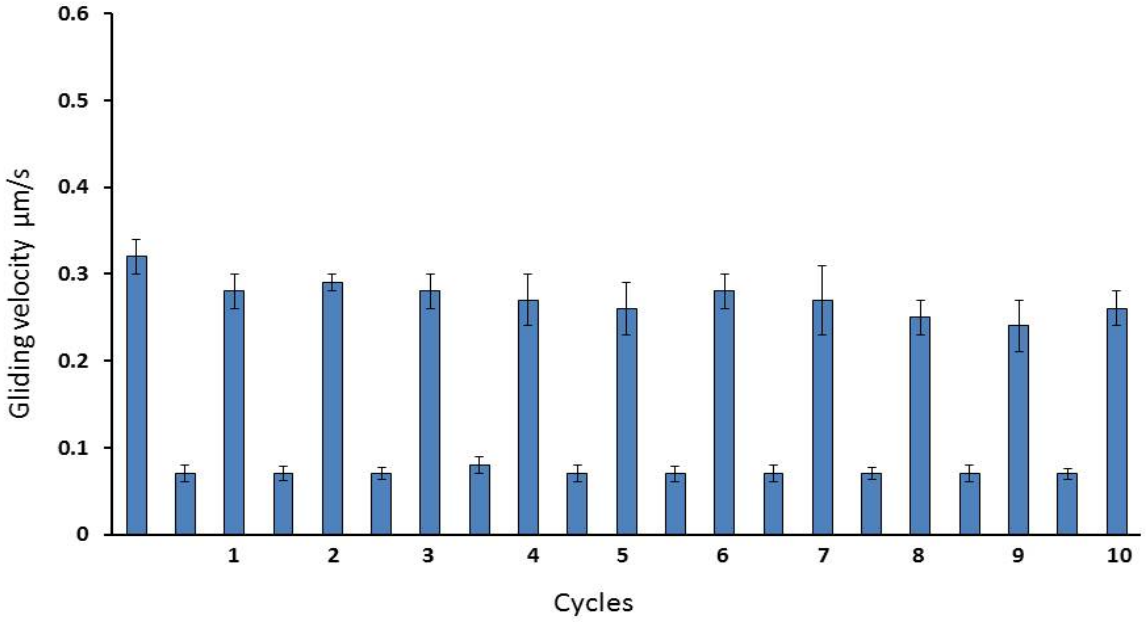

Figure 5: The repeatability in the photo-controllable gliding velocity change of AzoTP (3 mM) driven microtubules by alternative UV-Visible light irradiation over 10 cycles. The error bars represent standard deviations for 10 microtubules.

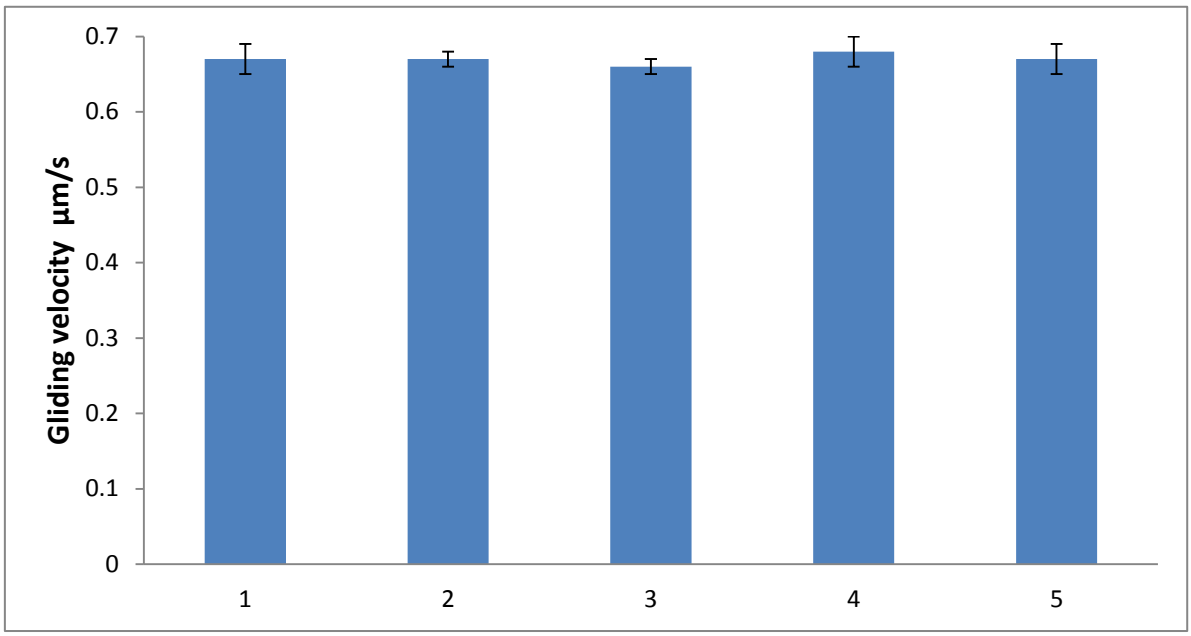

Figure 6: Kinesin-microtubule motility driven by 1 mM ATP as control experiment with alternate UV and visible light irradiation. 1) Before irradiation. 2) After UV (366nm) irradiation for 10 s. 3) After subsequent irradiation at 436 nm for 30 s. 4) After subsequent UV irradiation for 10 s. 5) After subsequent irradiation at 436 nm for 30 s. Error bars indicate standard deviation for 10 microtubules.

Figure 7 depicts the results of motility experiments performed with different concentrations of AzoTP in its non-irradiated and irradiated states. The red and blue circles indicate the gliding velocities corresponding to non-irradiated (100% *trans*) and irradiated (*cis*-rich) states, respectively. From 1H NMR spectra, we estimated that the *cis*-rich PSS contained 92% of the *cis* isomer and 8% of the *trans* isomer (**Figure 8**).

The black line in **Figure 7** indicates the microtubule gliding velocity predicted solely for the 8% content of the *trans* isomer; the measured gliding velocity for the *cis*-rich PSS was slightly higher than this line. Therefore, we estimated the contribution from the *cis* isomer (92% content) of AzoTP from the difference between the experimental velocities for the *cis*-rich PSS and the theoretical velocities (black line) for the *trans* isomer (8% content) of AzoTP. Accordingly, we found that the efficiency of the *cis* isomer for microtubule motility was only 1/29 of that of the *trans* isomer at an AzoTP concentration of 3 mM.

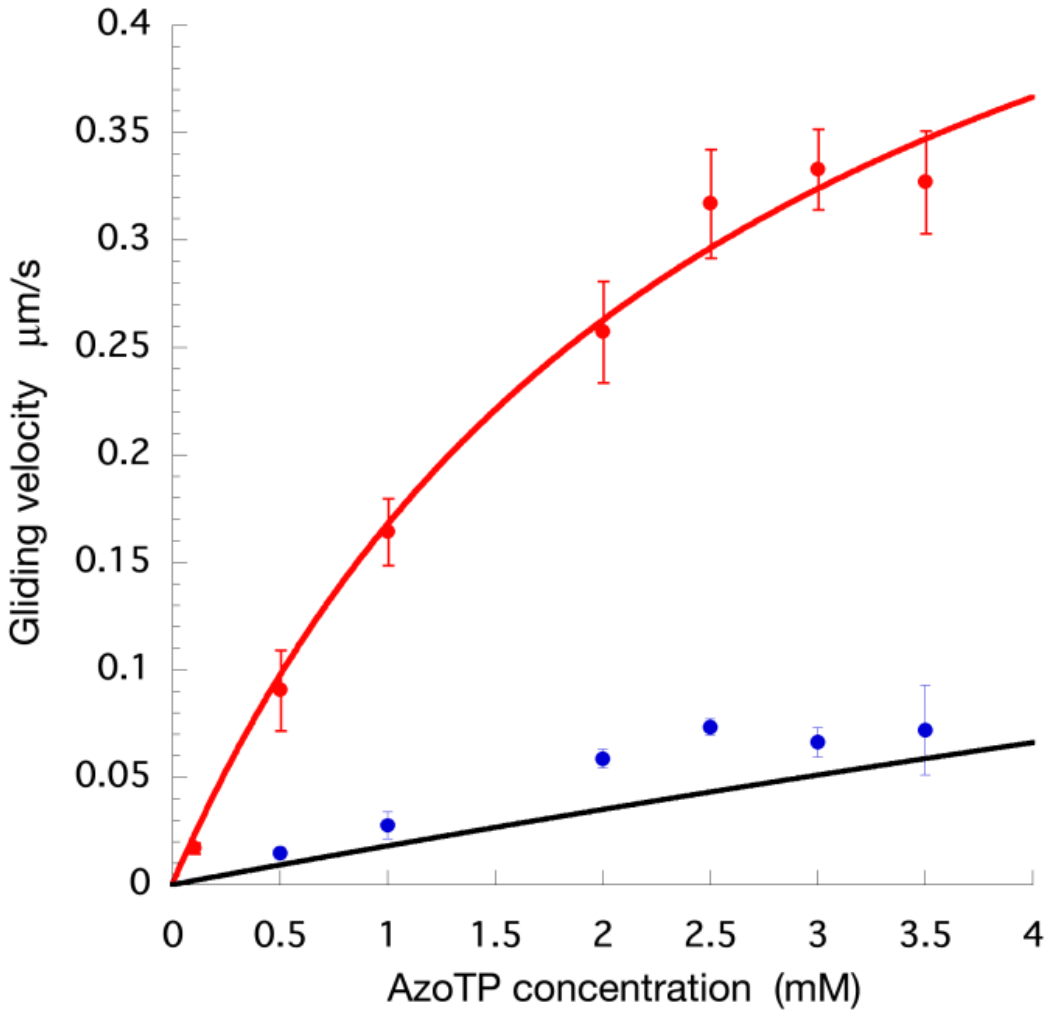

Figure 7 Concentration dependence curves of AzoTP on the gliding velocities of microtubules. Red circles are corresponding to observed gliding velocity for non-irradiated state. Red line represents the fitting curve by Michaelis-Menten equation (V_{max} = 0.61 µm/s and K_m = 2.6 mM). Blue circles are the observed gliding velocity for *cis*-rich states after 366 nm light irradiation. Black line is a theoretical curve derived from the red line for 8% of *trans* AzoTP. Error bars indicate standard deviations for 10 microtubules.

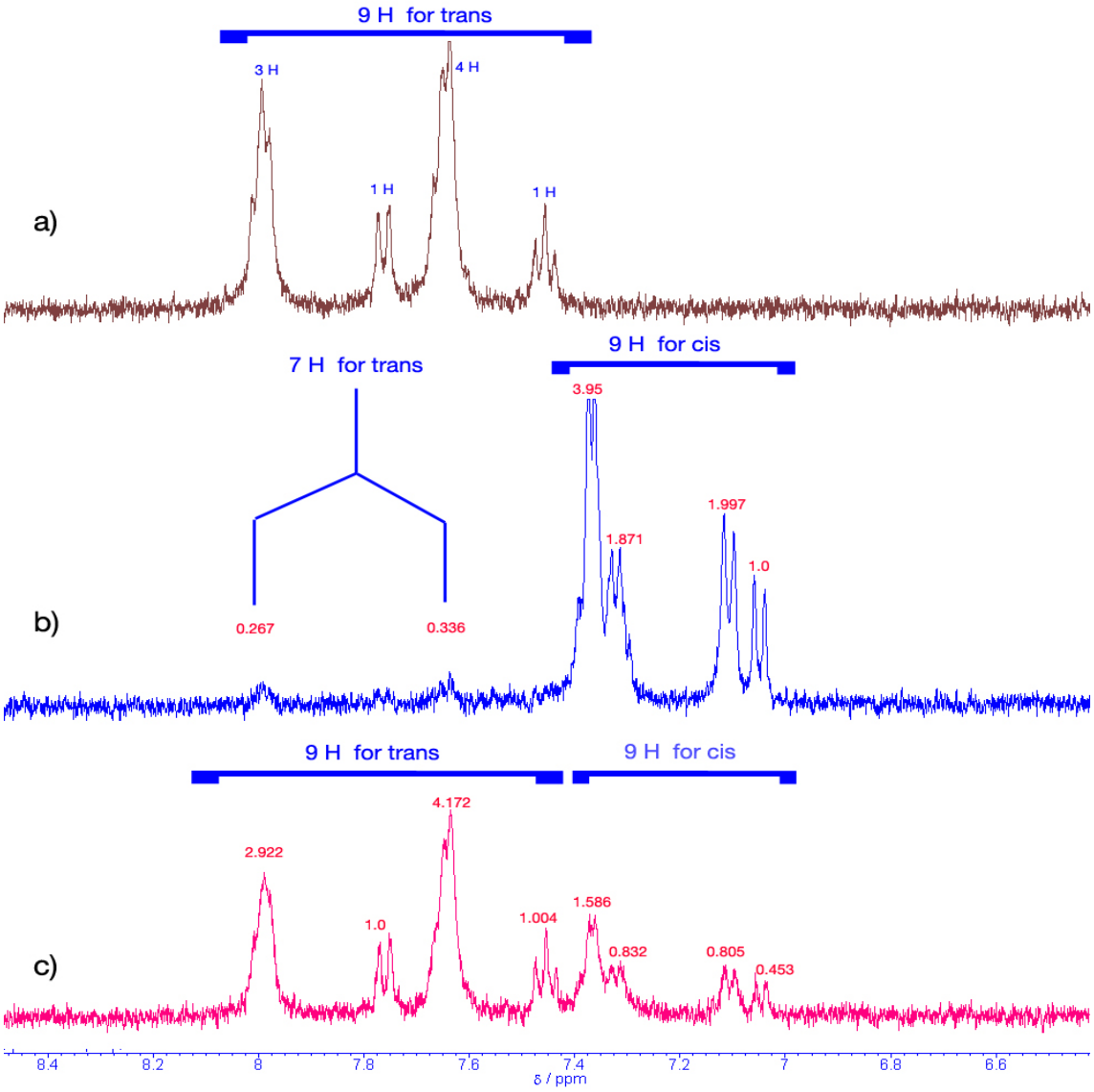

Figure 8: 400 MHz 1D ^{1}H NMR spectra of AzoTP in D_2O prior to irradiation (**a**), at 366 nm PSS (**b**) and at 436 nm PSS (**c**).The area of peaks at 7.45-8.02 ppm corresponds to 9 aromatic protons for trans AzoTP and at 7.05-7.39 ppm corresponds to 9 aromatic protons for cis AzoTP. The peaks at 7.61-7.68 and 7.97-8.02 ppm for 7 protons for trans isomer and the peaks at 7.05-7.39 ppm for 9 protons for cis isomer were used for the calculation of the trans/cis ratios 8/92 and 71/29 respectively.

The kinesin-microtubule system can be driven by several ATP analogues modified at its base or ribose unit[18] and by nucleoside triphosphates containing a variety of base units[29] (e.g., guanine, thymine, uracil, cytosine, inosine). In this present study, we have demonstrated that non-nucleosides can also be suitable replacements for the base and ribose units when preparing substrates for kinesin.

In sharp contrast to the performance of photoresponsive ATP derivatives substituted at the ribose moiety with a 4-*tert*-butylazobenzene unit,[23] AzoTP exhibits a quite large change in activity toward the kinesin-microtubule system upon photoisomerization. It has been established that the ribose group of ATP does not interact specifically with any of the amino acid residues of kinesin in the binding site, while the adenine unit is sandwiched through a stacking interaction with a histidine residue from below and through a hydrophobic interaction with a proline residue and the methylene group of an arginine residue from above.[30] The azobenzene moiety of AzoTP presumably plays a similar role as that of the adenine moiety of ATP. In its trans form, an azobenzene unit is flat, allowing it to undergo the stacking interaction found for ATP. In contrast, *cis*-azobenzene has a round shape that would prevent it from being sandwiched by the stacking and hydrophobic interactions. The large difference in activity of AzoTP in its *trans* and *cis* states can, therefore, be explained by considering

these differently shaped isomers experiencing different types of interactions in the binding site.

In summary, a new non-nucleoside triphosphate, AzoTP, allows substantial control over kinesin-microtubule motility−with a change in velocity of up to 79%−in a photoinduced and reversible manner.

3.2 Actomyosin motility assay.

Myosins,[4] a family of ATP-dependent linear-motor proteins move along actin filaments and are best known for their role in muscle contraction and their involvement in a variety of movements of non-muscle cells, including cell division, so these interactions play a central role in cell biology. The catalytic activity of myosin and actin-myosin-based motility systems have long been known to exhibit broad substrate specificity and many of the ATP analogues supported myosin mediated actin motility *in vitro*.[18]

In this study, we checked the motile properties of heavy meromyosin (HMM) in the translocation of actin filaments by utilizing non-nucleoside triphosphate, AzoTP, as fuel. We performed an in vitro acto-heavy meromyosin motility assay using the flow cell method.

Motility experiment shows that AzoTP drives actin filaments gliding with a saturated velocity (2.12 μm/s) at a concentration of 3 mM and this velocity is 62% of the saturated velocity driven by 0.3 mM of ATP (3.42 μm/s). **Figure 1** shows fluorescence images of gliding actin filaments after 0 and 5 s at 3 mM of AzoTP.

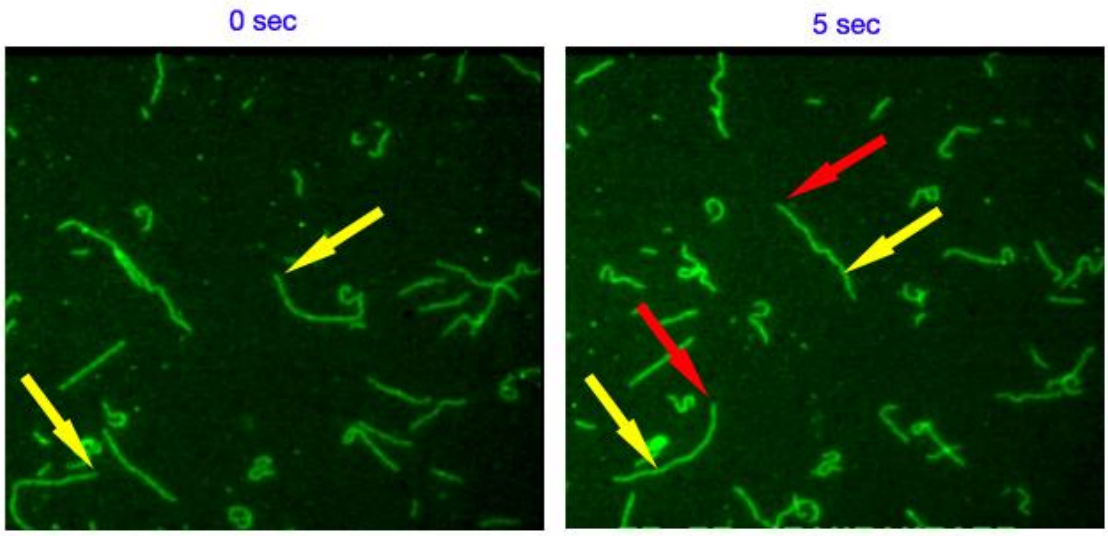

Figure 1. Fluorescence images of gliding actin filaments driven by AzoTP (3 mM) on heavy meromyosin adsorbed glass surface. (left) 0 s; (right) after 5 s in the flow cell. Yellow arrows: leading points of the actin filaments at 0 s; red arrows: leading points of the same actin filaments after 5 s.

Next, we carried out motility experiments with different concentrations of AzoTP. **Figure 2** indicates the concentration dependence of AzoTP on the gliding velocities of actin filaments and that obeys Michaelis-Menten kinetics. In the same manner, we carried out control experiments with different concentrations of ATP (**Figure 3**).

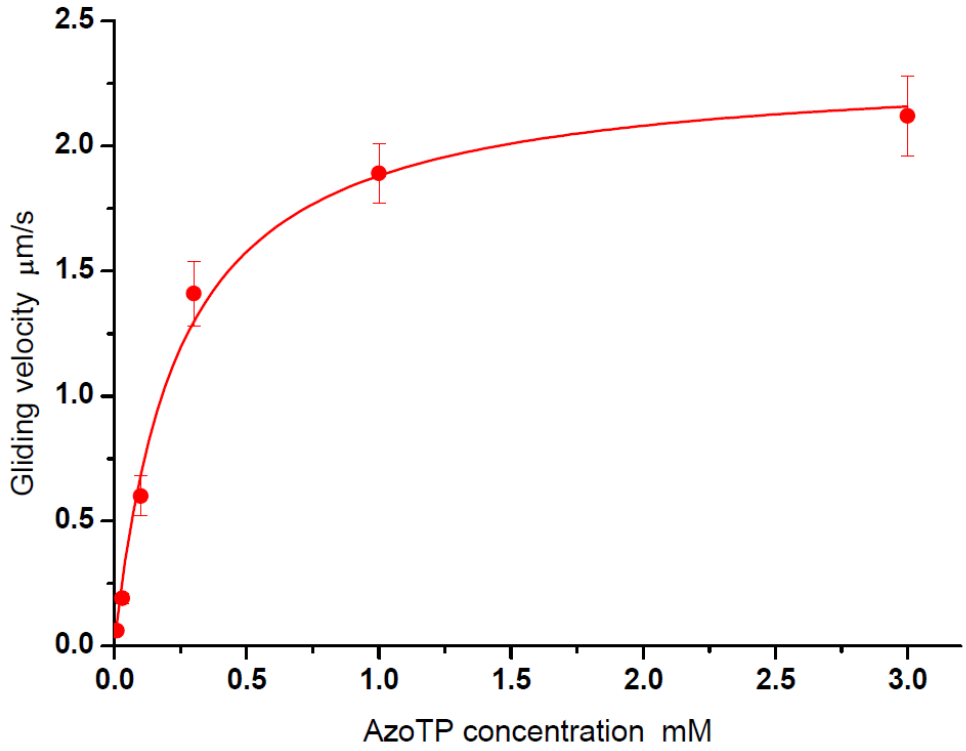

Figure 2. Gliding velocities of actin filaments plotted with respect to the concentration of AzoTP and the obtained curve fitted using the Michaelis-Menten equation (V_{max} = 2.33 µm/s; K_m = 0.24 mM). Error bars: Standard deviations for 10 actin filaments.

Figure 2 shows that **t**he maximum velocity (V_{max}) and Michaelis-Menten constant (K_m) are 2.33 µm/s and 0.24 mM, respectively. The Michaelis-Menten kinetic model provides K_m is an inverse measure of binding affinity towards the substrate. The obtained result shows that binding affinity of myosin motor protein towards AzoTP (ie., $1/K_m$= 4.17) was one-twelfth of the binding affinity of myosin towards ATP (ie., $1/K_m$ = 50.0). In case of kinesin motor protein, binding affinity towards AzoTP (ie., $1/K_m$ =

0.38) was one thirty-third of that of ATP (ie., $1/K_m$ = 12.5). These results indicate that binding affinity of myosin motor protein towards AzoTP was 11 times higher than that of kinesin.

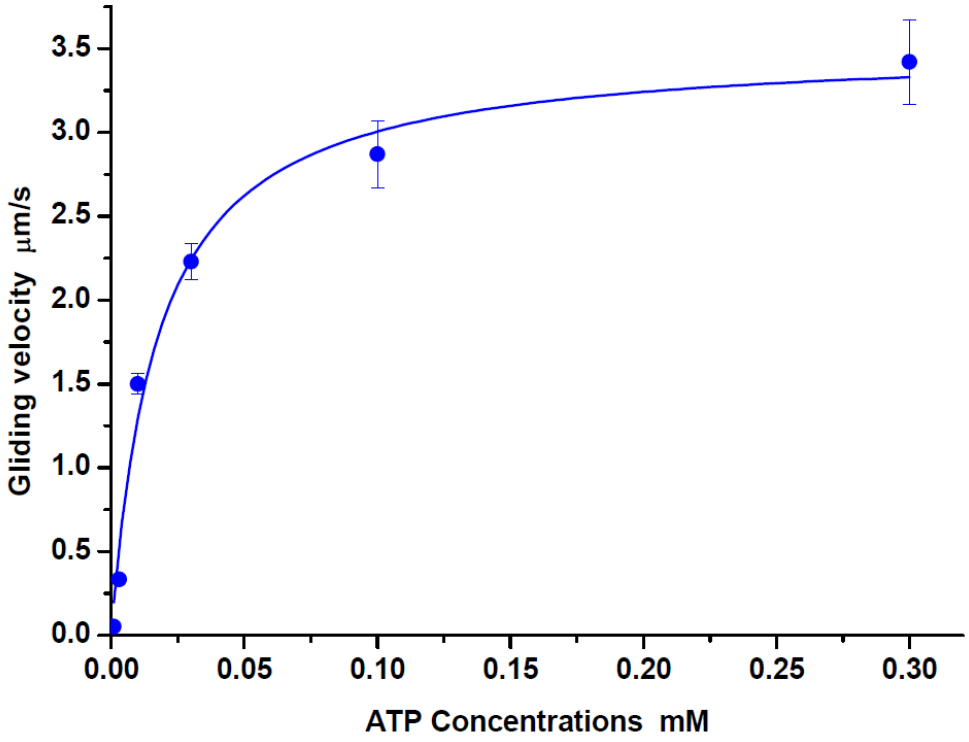

Figure 3. Gliding velocities of actin filaments plotted with respect to the concentration of ATP and the obtained curve fitted using the Michaelis-Menten equation (V_{max} = 3.52 µm/s; K_m = 0.02 mM). Error bars: Standard deviations for 10 actin filaments.

In summary, a new non-nucleoside triphosphate, AzoTP, drives actomyosin motility with 62% of the velocity of ATP driven motility. The binding affinity of myosin motor protein towards AzoTP was 11 times higher than that of kinesin.

3.3 F_1-ATPase rotation and hydrolysis assay.

The rotary motor protein, ATP synthase —also called F_oF_1 ATPase, or simply F-ATPase— is the central enzyme in energy conversion in mitochondria (where they are embedded into the mitochondrion's inner membrane), chloroplasts and bacteria.[5] ATP synthase terminates the biochemical process known as oxidative phosphorylation by synthesizing ATP from ADP and phosphate. This motor enzyme composed of two rotary motors, membrane integral F_o, which converts the proton motive force into rotation, and water-soluble F_1, which converts the rotation into synthesis of ATP. Remarkably, this process can be reversed in certain circumstances: F_1 component of ATPase can act as a biological motor, using up ATP in order to rotate its gamma sub-unit.

In this study, we investigated the hydrolysis activity and single molecular observation of rotation of F_1-ATPase using a non-nucleoside triphosphate, AzoTP, as a substrate. The hydrolysis activity was assessed as the amount of phosphate released by a colorimetric method[31] and single molecular observation of rotation assay with streptavidin coated polystyrene bead duplex was carried out under a phase contrast microscope.[32]

We carried out the single molecular observation of rotation assay of F_1 ATPase with a concentration of 1 mM AzoTP. We observed the rotation of polystyrene duplex

beads attached to the gama shafts of F1-ATPase at a concentration of 1 mM AzoTP (**Figure 1).** The four red lines indicate the time course of rotation of four different duplex beads in presence of 1 mM concentration of AzoTP.

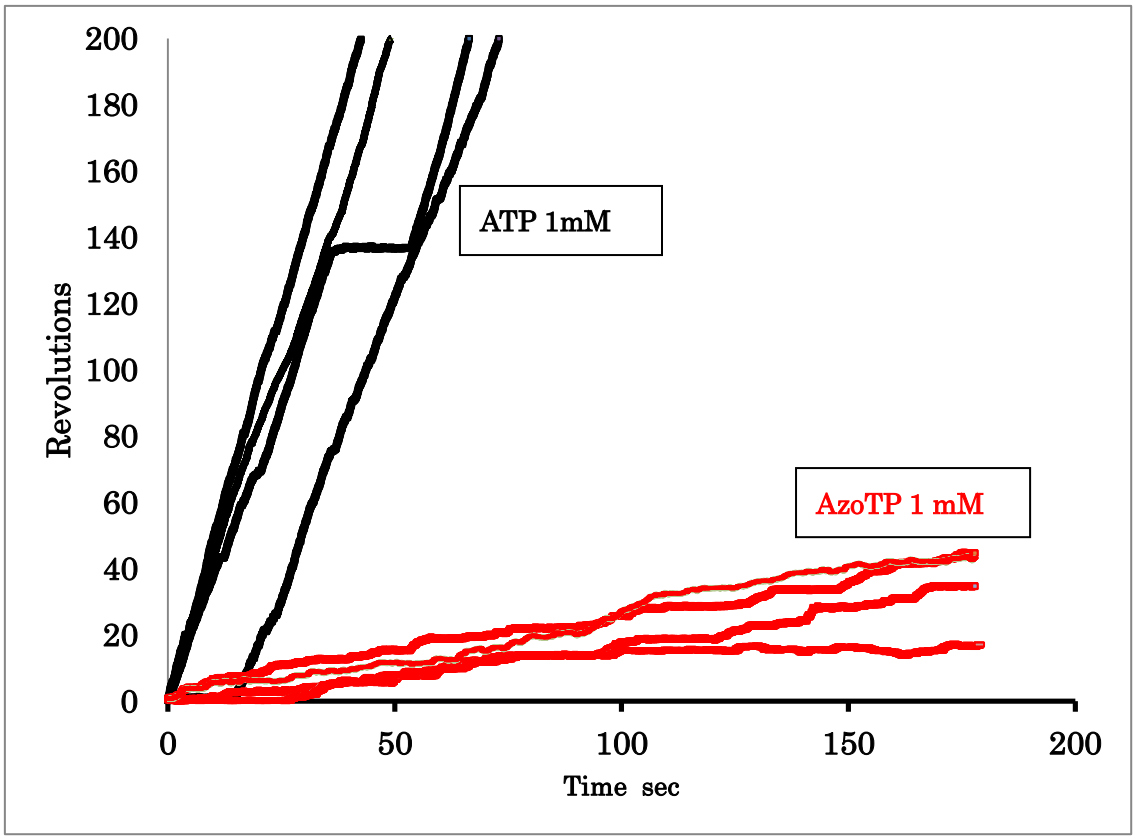

Figure 1. The time course of rotation of beads at 1 mM of ATP and AzoTP. The black and red lines indicate the rotation of beads at 1 mM of ATP and AzoTP in four different experiments, respectively.

The experiments for the measurement of hydrolysis activity revealed that AzoTP undergoes hydrolysis by the catalytic activity of F_1-ATPase. The obtained rate

constant, K_{cat}, for the hydrolysis activity at a concentration of 3 mM AzoTP was 0.65 s^{-1}, which is 1/100 times of that of ATP (66 s^{-1}).

Next, we investigated the effect of photoisomerization of AzoTP on the hydrolysis rate. We observed change in the concentration of phosphate formation upon alternating irradiation of UV and visible light at 0.9 mM of AzoTP (**Figure 2**). Hydrolysis activity was calculated from the obtained phosphate concentration for non-irradiated, UV and visible irradiated states. AzoTP provided K_{cat} of 0.34 s^{-1} at a concentration of 0.9 mM in its non-irradiated state. Direct UV irradiation (366 nm) converted *trans*-AzoTP to its *cis* form, thereby K_{cat} decreased to 0.03 s^{-1}. Subsequent irradiation with visible light (450 nm) led to increment in the hydrolysis rate (K_{cat}= 0.14 s^{-1}), due to *cis*-to-*trans* isomerization of AzoTP. **Figure 3** displays the changes in the hydrolysis rate upon alternating irradiation with UV and visible lights.

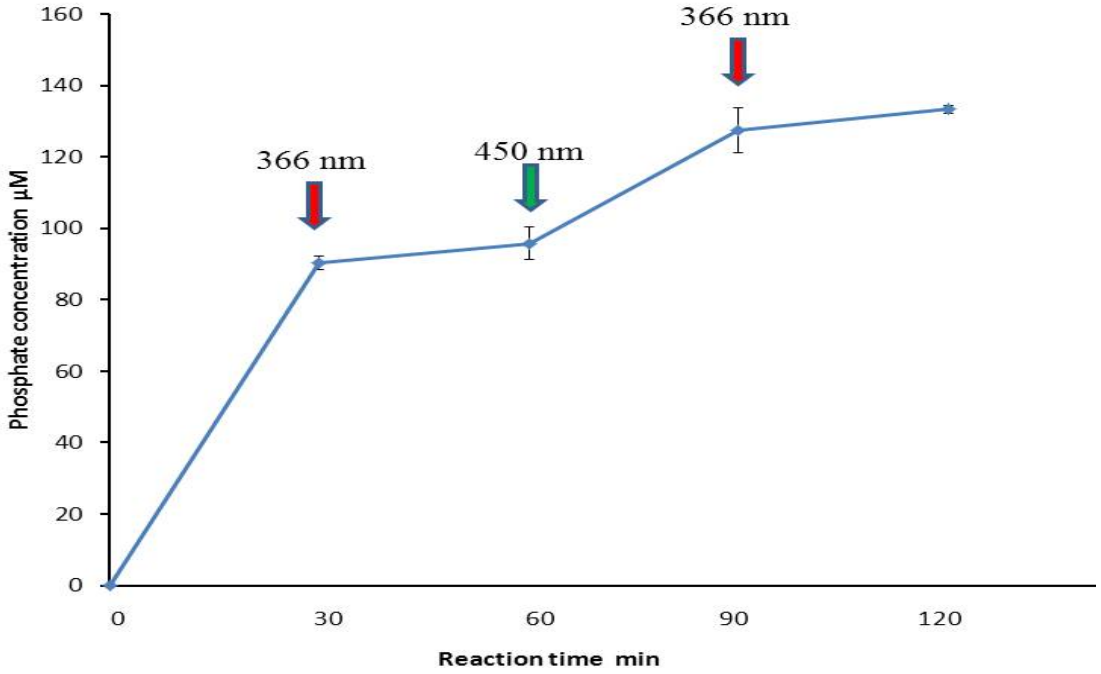

Figure 2. The effect of UV (366 nm) and visible light (450 nm) irradiation on the phosphate (Pi) formation during the hydrolysis of AzoTP (0.9 mM). Error bars represent standard deviations for 2 experiments.

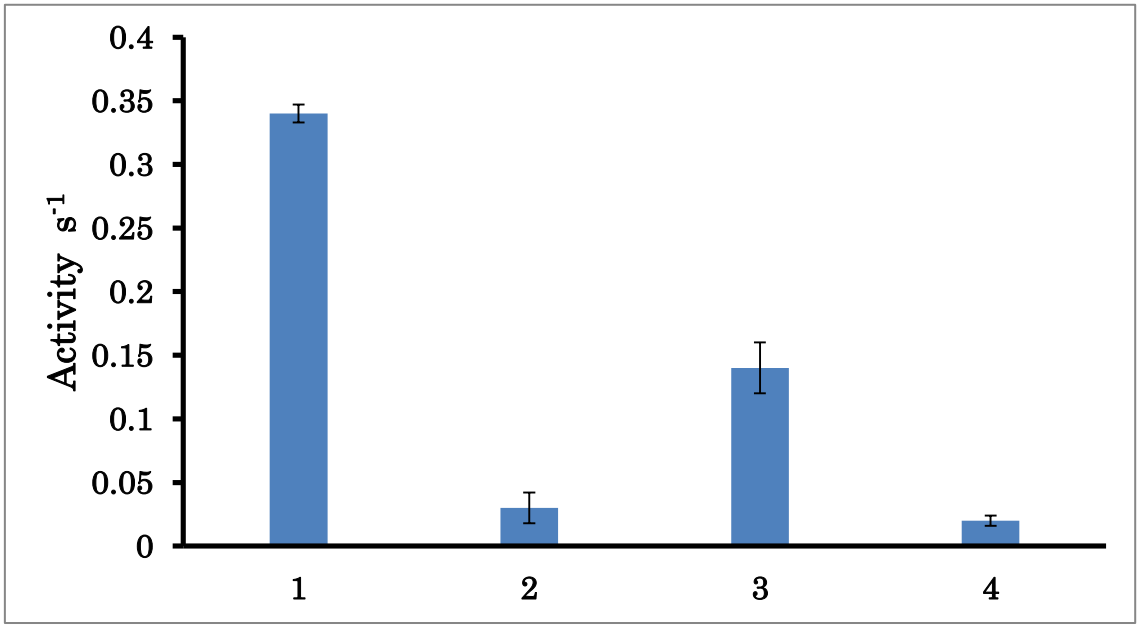

Figure 3. Changes in the hydrolysis activity of F_1-ATPase in the presence of AzoTP (0.9 mM) upon alternating irradiation with UV and visble light. 1) Before irradiation. 2) After UV (366nm) irradiation for 1 min. 3) After subsequent irradiation at 450 nm for 3 min. 4) After subsequent UV irradiation for 1 min. Error bars represent standard deviations for 2 experiments.

Figure 4 displays the hydrolysis activity of F_1-ATPase at different concentrations of AzoTP in its non-irradiated and irradiated states. The red and blue curves indicate the hydrolysis activity corresponding to non-irradiated (100% *trans*) and irradiated (*cis*-rich) states, respectively. The maximum decrease in the hydrolysis rate after photoirradiation of 3 mM of AzoTP was 88% of the initial hydrolysis rate of the *trans* form (**Figure 4**).

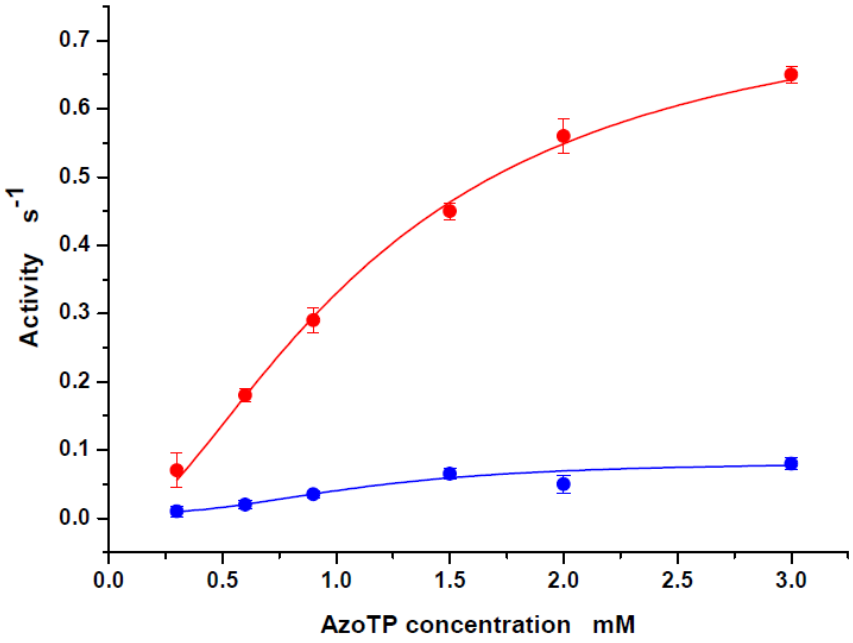

Figure 4. Hydrolysis activities of F_1-ATPase plotted with respect to the concentration of AzoTP. The red and blue lines indicate the hydrolysis activity in non-irradiated (100% *trans*) and irradiated (*cis*-rich) states, respectively.

In summary, we observed the single molecular rotation and hydrolysis activity of F_1-ATPase motor in the presense of AzoTP. The *cis*-to-*trans* photoisomerization of the azobenzene unit allows reversible and repeated control over the hydrolysis activity of F_1-ATPase.

4. Conclusion.

We synthesized a novel photoresponsive non-nucleoside triphosphate and used as a substrate to drive the motility of motor proteins. The obtained results suggested that AzoTP is generally active to motor proteins. The cis-trans photoisomerization of the azobenzene unit allows reversible and repeated control over the motility of motor proteins. This is the first demonstration of the substantial control of the activity of a motor protein in a reversible manner. It is expected that newly synthesized non-nucleoside triphosphate could be applied in biomotor-based transportation systems and in the artificial operation of natural motor proteins in living cells.

REFERENCES

1. M. A. Hoyt, A. A. Hyman and M. Bahler, *Proc. Natl. Acad. Sci. USA*, 1997, **94**, 12747.
2. S. T. Brady, *Nature*, 1985, **317**, 73; R. D. Vale, T. S. Reese and M. P. Sheetz, *Cell*, 1985, **42**, 39.
3. I. R. Gibbons and A. J. Rowe, *Science*, 1965, **149**, 424.
4. M. S. Mooseker and R. E. Cheney, *Annu Rev Cell Dev Biol*., 1996, **11**, 633.
5. P. D. Boyer, *Annu. Rev. Biochem*.,1997, **66**, 717.
6. S. G. Moorjani, L. Jia,T. N. Jackson and W. O. Hancock, *Nano Letters* 2003,**3**, 633; H. Hess, C. M. Matzke, R. K. Doot, J. Clemmens, G. D. Bachand, B. C. Bunker and V. Vogel, *Nano Letters*, 2003, **3**, 1651; H. Hess, G. D. Bachand, and V. Vogel, *Chemistry*, 2004, **10**, 2110; R. Stracke, K. J. Bohm, J. Burgold, H. J. Schacht and E. Unger, *Nanotechnology*, 2000, **11**, 52.
7. H. Liu, J.J. Schmidt, G.D. Bachand, S.S. Rizk, L.L. Looger, H.W. Hellinga, C.D. Montemagno, *Nat Mater.*, 2002, **1(3)**,173.
8. Y. Miyamoto, E. Muto, T. Mashimo, A. H. Iwane, I. Yoshiya, T. Yanagida, *Biophys. J*. 2000, **78**, 940.
9. H. Hess, J. Clemmens, D. Qin, J. Howard and V. Vogel, *Nano Lett.*, 2001, **1**, 235.

10. K. Aoki, M. Nakagawa, T. Seki, K. Ichimura, *J Am Chem Soc*, 2000, 122, 10997.

11. S. Kadota, K. Aoki, S. Nagano, T. Seki, *J Am Chem Soc*., 2005, **127**, 8266.

12. H. Yamamoto, A. Nishida, T. Takimoto and A. Nagai, *J. Polym. Sci., Part A: Polym. Chem.*, 1990, **28**, 67; K. Arai and Y. Kawabata, *Macromol. Rapid Commun.*, 1995, **16**, 875.

13. T. D. Ebralidze and A. N. Mumladze, *Appl Opt*., 1990, 29, 446.

14. M. K. A. Rahim, T. Fukaminato, T. Kamei and N. Tamaoki, *Langmuir*, 2011, **27**, 10347; M. K. A. Rahim, T. Kamei and N. Tamaoki, *Org. Biomol. Chem.*, 2012, **10**, 3321.

15. T. Kamei, T. Fukaminato and N. Tamaoki, *Chem. Commun.*, 2012, **48**, 7625.

16. N. Hirokawa, Y. Noda and Y. Okada, *Curr. Opin. Cell Biol*., 1998, **10**, 60.

17. N. Hirokawa and R. Takemura, *Nat. Rev. Neurosci*., 2005, **6**, 201.

18. R. D. Vale, *Cell*, 2003, **112**, 467.

19. T. Shimizu, K. Furusawa, S. Ohashi,Y. Y. Toyoshima, M. Okuno, F. Malik and R. D. Vale, *J. Cell Biol*., 1991, **112**, 1189.

20. T. Hiratsuka, *Biochim. Biophys. Acta*, 1983, **742**, 496.

21. For the one-way-control of the motility of kinesin by photochemical reactions: H. Higuchi, E.Muto, Y. Inoue and T. Yanagida, *Proc. Natl. Acad. Sci. U.S.A.*, 1997, **94,**

4395; H. Hess, J. Clemmens, D. Qin, J. Howard and V. Vogel, *Nano Lett.*, 2001, **1**, 235; A. Nomura, T. Q. P. Uyeda, N. Yumoto and Y. Tatsu, *Chem. Commun*., 2006, 3588.

22. T. Ikeda and T. Ube, Mater. Today, 2011, 14, 480; F. Ercole, T. P. Davis and R. A. Evans, *Polym. Chem.*, 2010, **1**, 37; N. Tamaoki and T. Kamei, *J. Photochem. Photobiol., C*, 2010, **11**, 47; T. Seki and S. Nagano, *Chem. Lett.*, 2008, **37**, 484; S. Yagai and A. Kitamura, *Chem. Soc. Rev*., 2008, **37**, 1520; K. G. Yager and C. J. Barrett, *J. Photochem. Photobiol., A*, 2006, **182**, 250.

23. M. Banghart, K. Borges, E. Isacoff, D. Trauner and R. H. Kramer, *Nat. Neurosci*., 2004, **7**, 1381; M. Volgraf, P. Gorostiza, S. Szobota, M. R. Helix, E. Y. Isacoff and D. Trauner, *J. Am. Chem. Soc.*, 2007, **129**, 260; S. Muramatsu, K. Kinbara, H. Taguchi, N. Ishii and T. Aida, *J. Am. Chem. Soc.*, 2007, **128**, 3764; M. D. Yamada, Y. Nakajima, H. Maeda and S. Maruta, *J. Biochem. (Tokyo)*, 2007, **142**, 691; B. Schierling, A. J. Noel, W. Wende, L. T. Hien, E. Volkov, E. Kubareva, T. Oretskaya, M. Kokkinidis, A. Rompp, B. Spengler and A. Pingoud, *Proc. Natl. Acad. Sci. U. S. A.*, 2010, **107**, 1361; F. Zhang, K. A. Timm, K. M. Arndt and G. A. Woolley, *Angew. Chem. Int. Ed.*, 2010, **49**, 3943; F. Bonardi, G. London, N. Nouwen, B. L. Feringa and A. J. M. Driessen, *Angew. Chem. Int. Ed*., 2010, **49**,

7234; C. Hoppmann, P. Schmieder, P. Domang, G. Vogelreiter, J. Eichhorst, B. Wiesner, I. Morano, K. Ruck-Braun and M. Beyermann, *Angew. Chem. Int. Ed.*, 2011, **50**, 7699; A. Mourot, M. A. Kienzler, M. R. Banghart, T. Fehrentz, F. M. E. Huber, M. Stein, R. H. Kramer and D. Trauner, *ACS Chem. Neurosci.*, 2011, **2**, 536.

24. For the one-way-control of the motility of kinesin by photochemical reactions: H. Higuchi, E.Muto, Y. Inoue and T. Yanagida, *Proc. Natl. Acad. Sci. U.S.A.*, 1997, **94**, 4395; H. Hess, J. Clemmens, D. Qin, J. Howard and V. Vogel, *Nano Lett.*, 2001, **1**, 235; A. Nomura, T. Q. P. Uyeda, N. Yumoto and Y. Tatsu, *Chem. Commun*., 2006, 3588.
25. D. Wang, E. Pate, R. Cooke and R. Yount, *J. Mus. Res. and Cell Motility*, 1993, **14,** 484.
26. M. E. Porter, J. M. Scholey, D. L. Stemple, G. P. A. Vigers, R. D. Vale, M. P. Sheetz and J. R. McIntosh, *J. Biol. Chem.*, 1987, **262**, 2794; J. Howard, A. J. Hudspeth and R. D. Vale, *Nature*, 1989, **342**, 154.
27. M. Castoldi and A. V. Popov, *Protein Expression Purif*., 2003, **32**, 83; J. Howard and A. A. Hyman, *Methods Cell Biol.*, 1983, **39**, 105.

28. The concentrations of AzoTP solutions were calculated based on the molecular weight of tetra sodium triphosphate. The error of the values of concentrations within 10% can be included due to the contamination of less sodium species (mono-, di- and tri-).

R. G. Yount, D. Babcock, W. Ballantyne and D. Ojala, *Biochemistry*, 1971, **10**, 2484.

29. S. A. Cohn, A. L. Ingold and J. M. Scholey, *J. Biol. Chem.*, 1989, **264**, 4290.

30. F. Jon Kull, E. P. Sablin, R. Lau, R. J. Fletterick and R. D. Vale, *Nature*, 1996, **380**, 550.

31. C. H. Fiske and Y. SubbaRow, *J. Biol. Chem.*, 1925, **66**, 375.

32. T. Nishizaka, K. Mizutani and T. Masaike, *Methods Mol Biol.*, 2007, **392**, 171.

LIST OF PUBLICATIONS.

1) Nishad Perur, Masao Yahara, Takashi Kamei and Nobuyuki Tamaoki "A non-nucleoside triphosphate for powering kinesin-microtubule motility with photo-tunable velocity"**,** *Chem. Commun.,* 2013**, 49**, 9935-9937.

2) Nishad Perur, Takashi Kamei, Ei-Ichiro Sunamura, Toru Hisabori, Taro Q. P. Uyeda and Nobuyuki Tamaoki "Activity and its change upon photoisomerization of a photochromic non-nucleoside triphosphate towards kinesin, myosin and F_1-ATPase" [To be submitted]

ACKNOWLEDGEMENT

Firstly, I owe my deepest gratitude to Almighty Allah, for His help and blessings to complete this research work.

This dissertation is completed first and foremost because of the support and ideas of my supervisor, Professor Nobuyuki Tamaoki. This work would not have been possible without his support, guidance and suggestions. Under his guidance I successfully overcame many difficulties and learned a lot. He provided me unflinching encouragement, financial support as well as one of the unforgettable research memories in my life. I would like to express deep sense of gratitude to him for giving me extraordinary experiences throughout the research.

I gratefully acknowledge Assistant Professors, Dr. Tsuyoshi Fukaminato and Dr. Takashi Kamei for their warm encouragement and involvement through important suggestion and discussions. Their help, advice and crucial contribution proved to be contagious and motivational for me, even during tough times of my Ph.D. I would also like to express my gratitude to Assistant Professor, Dr. Yuna Kim for her kind help and valuable suggestions.

I gratefully thank Dr. M. C. Basheer for his kind help and valuable discussions. I want to sincerely thank Dr. Reji Thomas, Dr. Oleksi Gutov, Dr. Mohammed Musthafa

T. N and Dr. Rika Ochi for their experimental co-operation and important discussions.

I am grateful to our group secretary Arisa Hirade and Mariko Ooki, they kept me organized and their indispensable help in dealing with scholarship and administration during my research so that I could optimally carry out my research and travels despite my poor ability to speak Japanese.

In my daily work I have been blessed with a friendly and cheerful group of fellow colleagues. I would sincerely appreciate and thankful all the members, Dr. Hashim P. K, Dr. Abdul Rahim M. K, Mr. Sunil Kumar K. R, Mr. Rijeesh K Nair, Miss. Halley M. M, Miss. Amrutha A. S, Mr. Islam Mohammed Jahirul, Mr. Akasaka T, Mr. Yukinari K, Mr. Yahara M, Mr. Nakamoto, Mr. Ito. S, Mr. Yoshida K and the technical assistant Miss. Tateyama E, for their kind supports and sacrificial help. I am grateful to them. I specially indicate Mr. Yahara M and Mr. Yoshida K for their experimental co-operation.

I would like to pay tribute to Hokkaido University, Japan for giving me the opportunity to study in Japan and learn the sweet culture of Japan. I wish to thank Dr. T. Q. P. Uyeda for providing me recombinant kinesin construct and actomyosin system. I wish to thank Prof. A. Kakugo for providing the lab instruments for the purification of protein specimen. I would like to thank Prof. Hisabori for providing F_1-ATPase assay

system and Dr. E. Sunamura for his experimental co-operation. I also want to express my sincere gratitude to Dr. P. Muhammed Ashraf (CIFT, Cochin) for his guidance and advice throughout my career. I would also like to thank all my teachers who gave me full support during my career.

I gratefully acknowledge the organization “JASSO (Japan Student Services Organization)” for giving me scholarship during my final year PhD course.

My family deserves special mention for their inseparable support and prayers. I would like to thank my whole family members including my parents Saidali P. and Biriyakutty C, my brothers Muhammed Ashraf P and Sidhique P.S, sister Seenath P, brother-in law Abdul Kareem K, sisters-in law Sajitha, Labitha and my beloved friends especially Abdul Rahman K, Abdul Hakeem K, Sajeer K and Yusuf Ali for their psychological support and encouragement during my career.

Last but not least, I would like to thank everybody who has been an important part in one or the other way for the successful realization of my thesis as well as my career. Finally, I am expressing my apology that I could not mention personally one by one.

Nishad Perur.